



CENTRO DE INGENIERIA Y DESARROLLO INDUSTRIAL

CAPACITIVE PRESURE SENSOR

# Dissertation

SUBMITTED IN PARTIAL FULFILLMENT OF THE REQUIEREMENTS  
FOR THE DEGREE OF

*Doctor in Science and Technology in*

*Design and Development of Mechanical Systems*

PRESENTS

005899

Francisco Romo Frias



Querétaro, Qro., México, 2009.



CIENCIA Y TECNOLOGÍA

2009

Director de Posgrado  
PICYT – CIDESI  
Querétaro

Los abajo firmantes, miembros del Jurado del Examen de Grado del alumno Francisco Romo Frias, una vez leída y revisada la Tesis titulada “ Capacitive Pressure Sensor ”, aceptamos que la referida tesis revisada y corregida sea presentada por el alumno para aspirar al grado de Doctor en Ciencia y Tecnología en la opción terminal de Diseño y Desarrollo de Sistemas Mecánicos durante el Examen de Grado correspondiente.

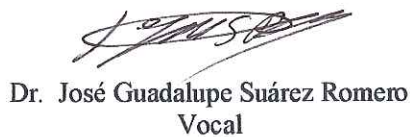
Y para que así conste firmamos la presente a los 2 días del mes de Octubre del año dos mil nueve.



Dr. Oscar Barceinas  
Presidente



Dr. Roberto Salas Zúñiga  
Secretario



Dr. José Guadalupe Suárez Romero  
Vocal



Dr. Álvaro Sánchez Rodríguez  
Vocal



Dr. Raúl Ramírez López  
Vocal

Director de Posgrado  
PICYT – CIDESI  
Querétaro

Los abajo firmantes, miembros del Comité Tutorial del alumno Francisco Romo Frías, una vez leída y revisada la Tesis titulada “Capacitive Pressure Sensor”, aceptamos que la referida tesis revisada y corregida sea presentada por el alumno para aspirar al grado de Programa de Doctorado en Ciencia y Tecnología en la opción terminal de Diseño y Desarrollo de Sistemas Mecánicos durante el Examen de Grado correspondiente.

Y para que así conste firmamos la presente a los 26 días del mes de Junio del año dos mil nueve.



Dr. Roberto Salas Zúñiga

Tutor Académico

Gerente General del Centro de Ingeniería y  
Tecnología, S.C



Dr Yingjie Lin

Tutor en Planta

Senior Staff Researcher Engineer  
Delphi Technologies, Inc. Troy Mich.

DEDICATION

For Martha, Alan and Jacqueline

and

Jesus<sup>†</sup> and Ma de la Luz

## TABLE OF CONTENTS

ACKNOWLEDGMENTS .....	6
ABSTRACT .....	7
LIST OF FIGURES .....	9
LIST OF TABLES .....	12
LIST OF SYMBOLS .....	13
<b>PART I. INTRODUCTION</b> .....	15
I.I PRIOR ART.....	15
I.II PROJECT DEFINITION.....	15
I.III JUSTIFICATION.....	17
<b>PART II. FUNDAMENTALS</b> .....	19
Chapter 1. General sensors.....	19
1.1 Introduction.....	19
1.1.1 Basic sensing.....	19
1.1.2 Types of sensors.....	20
1.2 Sensor characteristics.....	21
1.2.1 Transfer function.....	21
1.2.2 Accuracy.....	22
1.2.3 Resolution.....	23
1.2.4 Calibration.....	24
1.2.5 Hysteresis.....	24
1.2.6 Linearity.....	25
1.2.7 Saturation.....	25
1.2.8 Repeatability.....	26
1.2.9 Excitation.....	26
1.2.10 Dynamic characteristics.....	27
1.3 Principles of sensing.....	28
1.3.1 Capacitive.....	28
1.3.2 Magnetism.....	29
1.3.3 Inductance.....	30
1.3.4 Resistance.....	30
1.3.5 Piezoelectric.....	31
1.3.6 Optical.....	32
1.3.7 Resonance.....	32

Chapter 2. Capacitive Sensor.....	33
2.1 Introduction.....	33
2.1.1 Operational principle.....	34
2.1.2 Sensing element.....	34
2.1.3 Technical requirements.....	38
2.2 Applications/Current devices.....	39
<b>PART III. THEORY .....</b>	<b>42</b>
Chapter 3. The High Pressure Sensor.....	42
3.1 Introduction.....	42
3.1.1 Operational principle.....	42
3.1.2 Sensing element.....	44
3.1.3 Technical requirements.....	46
Chapter 4. Diaphragm .....	48
4.1 Introduction.....	48
4.2 Thin plate theory.....	48
4.2.1 Small deflection theory.....	48
4.3 Large deflection theory.....	53
4.4 Dynamic characteristics.....	55
4.5 Work done per pressure cycle.....	58
4.6 Residual stress.....	61
<b>PART IV. DESIGN .....</b>	<b>64</b>
Chapter 5. Electronic design.....	64
5.1 Schematic design.....	64
5.1.1 Layout.....	64
5.1.2 Predicted response.....	67
Chapter 6. Structural design.....	68
6.1 Diaphragm .....	68
6.1.1 Preliminary design.....	68
6.1.2 Predicted stress/deflection ratios.....	75
Chapter 7. Concepts generation.....	79
7.1 Mechanizations.....	79
7.1.1 Bill of design for concepts 1 to 7.....	82
<b>PART V. RESULTS AND DISCUSSION.....</b>	<b>86</b>
Chapter 8. Testing and experimental results.....	86
8.1 Highly Accelerated Test (HALT).....	86
8.2 Salt Fog.....	86
8.3 Vibration.....	86

8.4 Endurance.....	86
Chapter 9. Experimental results.....	
9.1 Performance.....	
9.1.1 Before design verification.....	
9.1.2 After design verification.....	
<b>PART VI. CONCLUSIONS</b> .....	<b>88</b>
Chapter 10. Optimization opportunities.....	88
Chapter 11. References.....	93
<b>APPENDICES</b> .....	<b>94</b>
Appendix A. High Pressure Sensor schematic .....	95
Appendix A. Patent No. US 7,383,737 B1.....	96
Appendix B. Technical Paper “Computational simulation for deflective diaphragm used on Capacitive Pressure Sensor”.....	105

## ACKNOWLEDGEMENTS

005899

There are two people who have made this dissertation possible; my two mentors Doctor Roberto Salas and Doctor Yingjie Lin were instrumental in all aspects of my endeavors, their guidance will remain with me as I continue my professional career.

In addition to early support in the form of formal education, my school CIDESI who has engaged me in thought giving the tools to understand the technological research of this project based on mathematical, simulation, materials science and statistical analysis. Most of the part of my technical education, administration and professional development is thanks to CIDESI.

Special thanks to everyone for their patience and the extra advice and work they did to produce pressure sensors prototypes: Dr. Oscar Barceinas who provided me with technical advice about material selection, Carlos Urquidi who actually was the designer of the electronic circuitry and Raul Damasco who helped to validate the prototypes; none of these devices could have been designed, fabricated and tested without them.

I thank Martha for her encouragement, patience and love who made the process of pursuing a Doctorate degree bearable. Finally, I thank to my two kids Alan and Jacqueline who have given me immeasurable support over these years.



## ABSTRACT

Capacitance sensing technology utilizes conductive electrodes to detect capacitance change corresponding to the relative position changes between the electrodes or the media physical property change between the electrodes. This kind of sensing skill is widely used for position/motion sensing (relative position change), acceleration sensing (gap changes between the electrodes), pressure sensing (gap change between electrodes), and chemical composition (media physical property change), etc

The present document presents a guideline for a pressure sensor design which minimizes the component count and simplifies the manufacture process besides the innovation in the sensing element architecture. In this design, there are two concentric electrodes placed on one side of a ceramic board. On the opposite, is the metal diaphragm which is chassis (or AC signal) ground. The two concentric electrodes with the AC ground form two capacitors. The gap between the diaphragm and concentric electrodes could be controlled by adding a step machined on top of the diaphragm or by adding a shim as extra component. Under zero pressure, the diaphragm has no deflection and the gap for the two capacitors is the same. If the area of the two concentric electrodes are designed as the same, then the two capacitance measurements are the same (in ideal case). Under pressure, the diaphragm is deflected like a dome: The center of the diaphragm has much larger deformation and results in a larger gap and the outer area has much less deformation and less gap change. The differential capacitance has good indication of the pressure. On the other hand, because of the sensor operation temperature change, the temperature coefficient of the gap material will cause the gap change too. For this temperature effects, it has the same effect on the two (the center and the outer) electrodes, the differential change is self-compensated (see US patent 7,383,737 B1 for detail).

### Structure of dissertation

The dissertation is divided into six parts and eleven chapters. The different parts cover the Introduction, Fundamentals, Theory, Design, Results and Discussion, Potential Optimization and Conclusions, everything belong the concept published in the Patent US 7,383,737 B1. If there are further optimization alternatives (modification to current High

Pressure Sensor) for the final design, will not be shown in this document due to Property Information disclosure.

In addition, each chapter has a synopsis which summarizes its content. There are also appendices which present additional theoretical background and detailed results.

## LIST OF FIGURES

- Fig 1-1. Accuracy of output signal for pressure sensor definition
- Fig 1-2. Saturation linear beyond linear output
- Fig 1-3. Repeatability for same sensor at same conditions
- Fig 1-4. Two parallel plates. Simplest capacitor array
- Fig 1-5. Hall element definition
- Fig 1-6. Wheatstone bridge configuration for strain gages sensing element
- Fig 2-1. Electric field between two charged conducting plates
- Fig 2-2. Electric field by Computational Simulation (ANSOFT) for symmetrical electrode's shape
- Fig 2-3. Round capacitor configurations
- Fig 2-4. Planar capacitor configurations
- Fig 2-5. Combined capacitor configurations
- Fig 3-1. Electric capacitance configuration
- Fig 3-2. Principle of operation. Capacitance at zero deflection.
- Fig 3-3. Principle of operation. Capacitance at diaphragm deflected
- Fig 3-4. Cross section view of diaphragm
- Fig 3-5. Electrodes arrangement on printing circuit board (PCB)
- Fig 3-6. Step ring provides the airgap (thickness)
- Fig 3-7. Sensing element assembly
- Fig 4-1. Graphical representation of the unit elongations in the x and y directions of an element lamina abcd at a distance z from the neutral surface
- Fig 4-2. Relation between Cartesian and polar coordinates.
- Fig 4-3. Normalized strain ( $Pa^2h/32D$ ) vs. normalized position for thin plate.
- Fig 4-4. a) Tensile forces per unit length N. b) Projection in radial direction of forces N and moments M uniformly distributed along the edge of the plate
- Figure 4-5. Corresponding stress ratio for small and large deflection theories.
- Figure 4-6. Coordinates transformation to Polar coordinates for circular plate calculation
- Figure 5-1. Flow process for capacitance measurement operating principle

Figure 5-2. Operating principle for electronic design  
Figure 5-3. Electronic layout for the HPS electronics  
Figure 5-4. Electronic layout for the HPS electronics  
Figure 5-5. Electronic layout for the HPS electronics  
Figure 6-1. Stress vs strain representation showing 40% of Yield to guarantee cycling endurance  
Figure 6-2. Notched tensile specimen showing location of fracture. SS 17-4 PH Heat treated 900 condition  
Figure 6-3. Cross section view of flat diaphragm  
Figure 6-4. DOE for flat diaphragm demonstrates that thickness is the main factor  
Figure 6-5. Annular Deformation Resistance Welding (ADRW) A) Diaphragm and B) Baseport configurations  
Figure 6-6. Annular Deformation Resistance Welding (ADRW) cross section view A) Detailed drawing interference and B) Prototype part  
Figure 6-7. Laser weld cross and plain views of prototype parts  
Figure 6-8 Preliminary assessment before run prototyping built for Machined and Stamped diaphragms  
Figure 6-9. Set up for proof of deflection test  
Figure 6-10. Predicted deflection at center of diaphragm based on FEA for not optimized diaphragm  
Figure 6-11. Predicted stress located at inner radius based on FEA for not optimized diaphragm  
Figure 6-12. Predicted thermal stress on overmold connector A)  $-40^{\circ}\text{C}$  and B)  $125^{\circ}\text{C}$   
Figure 7-1. QFD1 for HPS assembly  
Figure 7-2. QFD2 for HPS assembly  
Figure 7-3. Mapping FR's to DP's for HPS at sensor level  
Figure 7-4. A) Interconnection scheme. B) FEA for Option One  
Figure 7-5. A) Assembly scheme. B) FEA for Option Two  
Figure 7-6. A) Assembly scheme. B) FEA for Option Two  
Figure 7-7. A) Assembly scheme. B) FEA for Option Two  
Figure 7-8. A) Interconnection scheme. B) FEA for Sheet metal diaphragm Option Six

- Figure 7-9. Interconnection scheme for Option Seven for Step and Flat diaphragm
- Figure 7-10. Pugh analysis for HPS concept selection against Datum (Potential supplier)
- Figure 8-1. Compensated and linearized HPS output @ Temperature
- Figure 9-1. Axiomatic Design. Functional Attribute Analysis HPS
- Figure 9-2. Ideal Function for diaphragm deflection optimization
- Figure 9-3. P-Diagram including Constraints and Unwanted Outputs
- Figure 9-4. Step diaphragm used on early stages of proof of concept
- Figure 9-5. Flat diaphragm and shim option used on final design

## LIST OF TABLES

Table 1. Technical requirements for HPS 3000 PSI

Table 2. Numerical comparison between FEA and two different real parts

Table 3. Predicted thermal growth values

Table 4. Optimization confirms, but does not provide sufficient deflection (Beta)

## LIST OF SYMBOLS

Logarithmic function:  $S = a + b \ln s$

Exponential function:  $S = ae^{ks}$

Power function:  $S = a_0 + a_1 s^k$

$$\text{Capacitance } C = \iint \epsilon_r \epsilon_0 \frac{dx dy}{z(x, y)}$$

$\epsilon_r$  is the media relative dielectric constant (for air, it is very close to 1).

$\epsilon_0$  is the dielectric constant of vacuum ( $8.85E-12$  F/m)

$Z(x, y)$  is the gap distance between the electrodes.

$$\text{Inductance } V = -L \frac{\partial I}{\partial t}$$

$L$  is the inductance in units of henrys. The minus sign indicates that the voltage (V) opposes the change in current (I).

$$R = \rho \frac{l}{a} = \frac{m}{n \cdot e^2 \cdot \tau} \frac{l}{a}$$

$l$  is the length

$a$  is the area or cross section of the conductor

$\rho$  is the resistivity of the material

$\tau$  The resistivity of a material through mean time between collisions

$e$  the electronic charge

$m$  the mass of electron

HPS	High Pressure Sensor
IC	Integrated Circuit
ADRW	Annular Deformation Resistance Welding
DFSS	Design For Six Sigma
BOD	Bill Of Design
QFD	Quality Function Deployment
FR	Functional Requierements
s/n	Signal to Noise ratio

$\gamma_{rz} \gamma_{\theta z}$	Shearing stress
$\epsilon_r$	Radial strain
$\epsilon_\theta$	Circumferential strain
$\sigma$	Mechanical Stress
$u$	Radial stretch
$\nu$	Poisson's ratio
$E$	Elastic modulus
$P$	Applied pressure
$a$	Disc area
$D$	Diameter
$H$	Thickness of plate
$r$	Radial position
$V_1$	Energy of bending
$V_2$	Energy due to stretching
$U$	Radial displacement
$C_1$ and $C_2$	Integration constants
$w_0$	Maximum Deflection
$\rho$	Density
$T$	Kinetic energy
$p$	Frequency of circular plate clamped at the boundary
$p_1$	Frequency of the lowest mode of vibration



## PART I. INTRODUCTION

### I.I PRIOR ART

In industry, a pressurized deposit/system is commonly used to provide pressurized fluid to a hydraulic system. This pressure must not exceed the operation range to guarantee correct functionality and does not compromise the integrity of the system and avoid damages to the final user.

Currently in the market there are several technologies for pressure measurement based on sensors alternatives. The piezoresistive technology implemented using thick film, thin film and MEM's building a strain gage placed on top of a sensing membrane and capacitive technology on MEM's and discrete membranes.

The present document, describes the use of a well know method for capacitance measurement and introduces a more simple manufacturability of the sensing element without compromising the sensor performance and with the flexibility to use the same sensing structure for a wide range of pressures and applications without the media compatibility problem of the sensing membrane. The electrodes arrangement is the other innovation of this sensor which makes not a particularity compared with the other designs.

### I.II PROJECT DEFINITION

The scope of this dissertation is limited over the mechanical design of the deflective diaphragm and final mechanization for the Capacitive Pressure Sensor. Even when a short description of the electronic circuitry is included as well, its design is under information property for Delphi Technologies and Analog Devices.

Furthermore, the framework that was used to develop this dissertation integrates most of the tools that were used during the development of the Capacitive Pressure Sensor and

actually ties together all of the conducted stages since technology identification onto proof of concept to end up with an optimized design for robustness.

The capacitive effect is the ability of a pair of electrodes to hold an electric charge which is widely used for many sensing device. One of the alternative designs is the Capacitive Pressure Sensor which senses variation in pressure as described in Patent US 7,383,737 B1.

The work reported in this dissertation is established in three major areas:

1. Descriptive of innovation in the capacitive sensing cell
2. Baseline consideration for the Capacitive Pressure Sensor design
3. Proof of concept

1. Descriptive of innovation in the capacitive sensing cell

There are two round electrodes printed on one side of a ceramic board electrically connected to electronic components on top of same board. At front of those two electrodes there is a metallic diaphragm that deflects according to a pressure variation. There is also an air gap that is created by including a shim or a machined step on top of diaphragm. Several technical literatures have published the characteristics of the metallic diaphragms under uniform load and clamped edges that actually measure the deflection in a dome shape for application to pressure sensors

2. Baseline consideration for the Capacitive Pressure Sensor design

The baseline recommendations are important factors to guide the design end with good and robust diaphragm establishing the understanding of the baseline and design recommendations to simulate and calculate a flat metallic deflective diaphragm. The maximum diaphragm deflection becomes significantly important for the dynamic range of the sensor. This deflection can be easily predicted based on FEA simulation models. The main considerations to conduct these simulations are related to material properties, boundary conditions and geometry of the diaphragm. Beside the simulations; statistical analysis plays an important role to understand the behavior and impact of different combinations between the design factors.

A recommended electronic layout, diaphragm design and packaging mechanization are also presented by the end of the document for High Pressure Sensor 500 and 3000 PSI for DIG application.

### 3. Proof of concept

Along the design stage of the sensor, there are noises that cannot be anticipated or controlled. Unfortunately these noises decrease the confidence level of the product and may carry warranty issues. That is why the product needs to be tested at different harsh conditions before release to production, however for those noises that can be anticipated (even occasionally), must be included during the design stage in order to end up with a robust design. One of them is the batch to batch variation in material properties that can be physically difficult in practice to determine an exact value. Otherwise, it is recommended to take a historical mean value using a statistical sample. A good sensing element design should compromise the signal level and the fatigue/safety concerns.

## I.III JUSTIFICATION

A sensor is a device that transfers physical quantity to electrical signal, such as voltage, which could be read by human or control unit. Pressure sensor is used to “sense” either absolute or differential pressure of a pneumatic or hydraulic system. For automotive industrial, those systems include fuel system, ABS, engine, etc.

Creation of sources of revenues based on development of new products are always an important factor for the continue growth of any company based on technology innovation. Even more when there is a need to provide a reliable product to satisfy the technical/cost needs of a potential costumer.

The successful launch of any new sensor project will depend of those characteristics that are oriented to enhance its use with a competitive price, robust design and innovation in technology. Few brand names are dominating the automotive pressure sensor market. Currently, each one has its own design according to the technology of the sensing element and manufacturability process.

There are two kinds of pressure sensor: One is called absolute sensor which has a vacuum cell (ZERO pressure) on one side of the diaphragm as the reference to measure the absolute pressure. The other is called gauge sensor which measures the pressure difference across the both sides of the diaphragm.

The mathematical modeling and computer simulation are the most powerful tools to be used from the beginning of concept part design to the final product optimization. These tools could help us significant shorting the design iteration, reducing the prototype build/test costs. By changing the simulation condition, such as: temperature, pressure, etc., the results could help us to understand what may happen at normal operation and at the extreme condition without really built and test the part.

## PART II. FUNDAMENTALS

### Chapter 1. General sensors

#### 1.1 Introduction

A sensor is a device that provides a translation of a physical phenomenon into an electrical output to enhance the operation of a system. The principle of operation of any sensor is the conversion of energy, so its design may be for general use or selective purpose, that will depend of the complexity to convert that energy and packaging design. In automotive industry there are several systems and furthermore applications such as pressure inside a pressurized container/line, chassis leveling, level of fuel tank, humidity detection, oil degradation, etc.

Some cases a sensor is erroneously called transducer; however the transducer is the device that converts energy into another different such as a speaker that converts electricity into acoustic waves.

##### 1.1.1 Basic sensing

A sensor is called a device that converts a physical phenomenon into an electrical output signal. There are several classifications schemes to group a sensor device, however the most practical way to look at are two kinds [4]

1. Passive sensor: These devices do not need any operation or signal condition energy source and directly generates an electric signal in response to an external stimulus. The examples are a thermocouple, a photodiode, and a piezoelectric sensor.

2. Active sensor: These devices require external energy source to maintain the operation. The signal is modified by the sensor to produce the output response. The active sensors sometimes are called parametric because their own properties change in response to an external effect and these properties can be subsequently converted into electric signals. For example, a thermistor and a strain gauge. They do not generate any electric signal, but by passing an electric current through it (excitation signal), its resistance can be measured by detecting variations in current and/or voltage across their body.

#### 1.1.2 Types of sensors

The field of application is wide extensive, and actually the same concept may be used for two or more applications (depending on technical requirements). Those applications are more oriented to automotive, manufacturing, health, military, energy, transportation, agriculture, domestic, aerospace and other. But according to their conversion phenomena [4] the sensors can be classified as:

##### Physical

- Thermoelectric
- Photoelectric
- Photomagnetic
- Magnetolectric
- Thermoelastic
- Electroelastic
- Thermomagnetic
- Thermooptic
- Photoelectric
- Other

## Chemical

- Chemical transformation
- Physical transformation
- Electromechanical process
- Spectroscopy
- Other

## Biological

- Biochemical transformation
- Physical transformation
- Effect on test organism
- Spectroscopy
- Other

### 1.2 Sensor characteristics

A sensor data sheet is the numerical/graphical attributes of the characteristics and performance of the sensor under particular conditions and specific applications and will depend of the physical nature. Some of the most important sensor performance characteristics are described bellow [4, 7].

#### 1.2.1 Transfer function

The mathematical (ideal or theoretical) function that exists for every sensor and mathematically relates the input stimulus and the output signal and can be represented graphically as the dependency between the electrical output signal produced by the sensor and the input stimulus. This graphic representation is called most of the time as calibration curve too. Depending on the technology used and if the stimulus is influenced by other stimulus, the transfer function can be linear or nonlinear. When there is linear output, the output function is simple to compute, however when it is nonlinear, it becomes more complex and a mathematical approximation method can be used to fits well the transfer function

A one-dimensional linear relationship is represented by the equation  $S = a + bs$  where  $a$  is the intercept (i.e., the output signal at zero input signal) and  $b$  is the slope, which is sometimes called sensitivity.  $S$  is one of the characteristics of the output electric signal used by the data acquisition devices as the sensor's output.

Logarithmic function:  $S = a + b \ln s$

Exponential function:  $S = ae^{ks}$

Power function:  $S = a_0 + a_1 s^k$

where  $k$  is a constant number.

To determine whether a function can be represented by a linear model, the incremental variables are introduced for the input while observing the output. A difference between the actual response and a linear model is compared with the specified accuracy limits. For a nonlinear transfer function, the sensitivity  $b$  is not a fixed number as for the linear relationship. At any particular input value,  $s_0$ , it can be defined as

$$b = \frac{dS(s_0)}{ds}$$

Piecewise approximation: A nonlinear sensor may be considered linear over a limited range. Over the extended range, a nonlinear transfer function may be modeled by several straight lines.

When output is influenced by more than one stimulus, a transfer function may have more than one dimension; an example is a thermal radiation sensor (infrared).

### 1.2.2 Accuracy

The closeness of agreement between a test result and accepted reference value [19]. The term accuracy, when applied to a set of test results, involves a combination of random components and a common systematic error or bias component.

Observed value: the value of a characteristic obtained as the result of a single observation.

Test result: The value of a characteristic obtained by carrying out a specified test method.



**Bias:** the difference between the expectation of the results and accepted reference value. Is the total systematic error as contrasted to random error. There may be one or more systematic error components contributing to the bias. A larger systematic difference from the accepted reference value is reflected by a larger bias value.

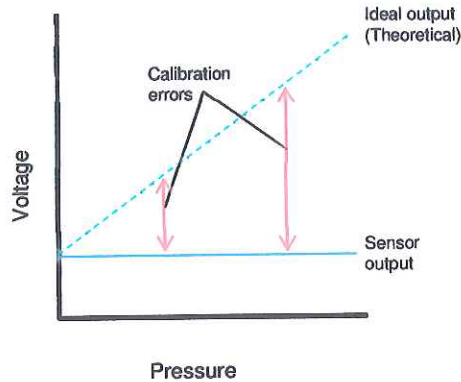


Fig 1-1. Accuracy of output signal for pressure sensor

Based on the figure above; accuracy is a qualitative value that expresses how much deviation is the reading of the sensor from the true value and shows a dependency of the transfer function. It can be explained as the sum of linearity, hysteresis and repeatability at room temperature. A device may be very linear, have low hysteresis and high repeatability, but still produces an output unrelated to the input pressure because it is not calibrated well because of the error band.

### 1.2.3 Resolution

The resolution of a sensor is the smallest reliable measurement that the sensing element is capable to detect. The resolution of a measurement must be better than the final accuracy the measurement requires.

The primary determining factor of resolution is electrical noise. The electrical noise appears and causes small errors in the output even when the system is perfectly constant; the electrical noise can only be minimized and never eliminated.

Sensor data sheets generally quote resolution in units of signal/root (Hz) but for some cases, the resolution may be as percentage of full scale due to variation under specified

noises conditions. Otherwise, the sensor has a smooth output signal and has continuous or infinitesimal resolution.

#### 1.2.4 Calibration

Physical equivalence between the mathematical model of the transfer function and the change of stimulus [20].

Sensitivity. Indicates how much the output voltage changes as a result of a change in the gap between the target and the sensor. A common sensitivity is  $1V/0.1mm$ . This means that for every 0.1mm of change in the gap, the output voltage will change 1V.

Bandwidth. The frequency at which the output falls to -3dB. This frequency is also called the cutoff frequency. A -3dB drop in the signal level equates to approximately 70% drop in actual output voltage.

The sensor is calibrated at different known values (pressure, distance, etc). The measurements at these points are collected and the sensitivity and linearity are analyzed by the calibration system. The analysis of the data is used to adjust the system being calibrated to meet order specifications. After sensitivity and linearity are calibrated, the capacitive sensor systems are placed in an environmental chamber where the temperature compensation circuitry is calibrated to minimize drift over the temperature range. During calibration in factory there is a calibration error that is of a systematic nature and is permitted by a manufacturer and may impact the overall accuracy.

#### 1.2.5 Hysteresis

When the input stimulus is cycled the sensor output does not have the same value but depending upon the "history" of the stimulus input. For same stimulus input level, say level A, the sensor may output B1 if the stimulus was increased from lower level to A, and the sensor may output B2 if the stimulus was decreased from higher level to A. The difference between B1 and B2 is called the "hysteresis" of the sensor.

Typical causes for hysteresis are friction and structural changes in the materials.

### 1.2.6 Linearity

The measurement of the straightness of the line and not the slope of the line. Linearity is the maximum deviation from a linear transfer function over dynamic range. Independent linearity is referred to as the so-called “best straight line” which is a line midway between two parallel straight lines closest together and enveloping all output values on a real transfer function.

Linearity Error. Sensitivity can vary slightly between any two points of data. The accumulated effect of this variation is called linearity error. The linearity specification is the measurement of how far the output varies from a straight line. A system with gross sensitivity errors can be very linear [20].

To calculate the linearity error, calibration data is compared to the straight line that would best fit the points. This straight reference line is calculated from the calibration data using a technique called least squares fitting. The amount of error at the point on the calibration line that is furthest away from this ideal line is the linearity error. Linearity error is usually expressed in terms of percent of full scale.

### 1.2.7 Saturation

Some technologies do not exhibit more response (or desirable) when it reaches certain level of input stimulus even when its transfer output is linear. This effect is said that the sensitive element reaches its operating limit and its output signal no longer will be responsive.

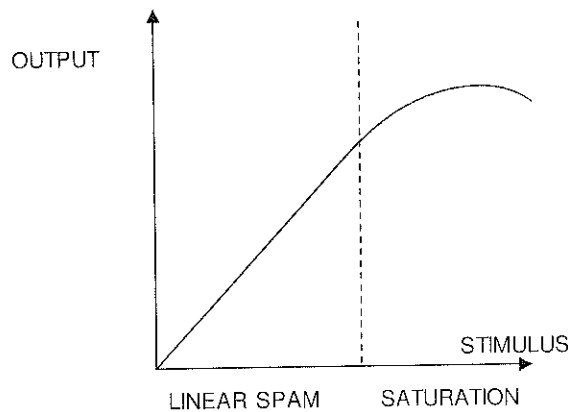


Fig 1-2. Saturation linear beyond linear output

### 1.2.8 Repeatability

Repeatability is the ability of a sensor to reproduce the same results under the same testing conditions all time. These conditions must also include the same level of noises.

The absolute difference between two independent single test results, obtained using the same method on identical test material in the same laboratory by the same operator using the same equipment within a short interval of time.

Repeatability error [20]: Is the deviation in output readings for successive applications of any given input pressure with other conditions remaining constant.

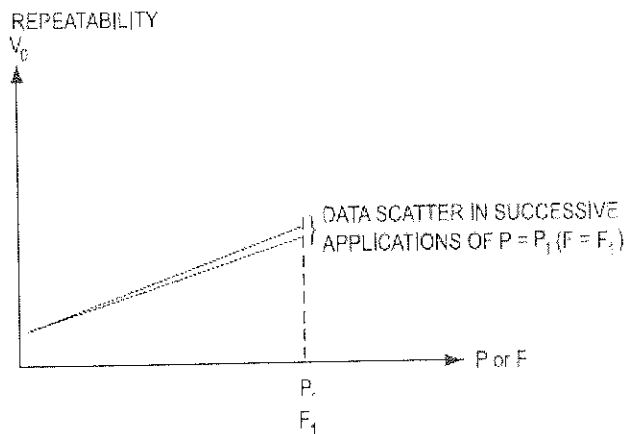


Fig 1-3. Repeatability for same sensor at same conditions

### 1.2.9 Excitation

Is the electrical signal necessary to active the sensing element to desirable operation.

The type of output desired might determine the excitation voltage that is needed [20].

Many sensors assembly (final design) have built-in voltage regulators and will operate over a wide range of voltages from an unregulated power source. Ratiometricity implies

the sensor output is proportional to the supply voltage with other conditions remaining constant.

Ratiometricity error is the change in this proportion and is usually expressed as a percent of Span. It is desirable to obtain a linear relationship between the excitation and output signal (Transfer function).

#### 1.2.10 Dynamic characteristics

- Warm up time or time response: Is the time that a sensor takes to operate and become fully operational and accurate.
- Response speed: How fast the sensor can response to a physical stimulus
- Damping: Is the suppression of the oscillation in the response of a sensor
- Cutoff frequency: Indicates the lowest or highest frequency of stimulus that the sensor can process.
- Phase shift: At a specific frequency defines how the output signal lags behind in representing the stimulus change
- Dynamic range: Is the difference between the highest and lowest readings of a linear transfer function.

## 1.3 Principles of sensing

As previously mentioned, there are two kinds of sensing devices (passive and active). However, it may be also a potential classification that is more related to the physical phenomena [7]:

- Contact sensors: Require a physical interface between the stimulus and the sensing device.
- Noncontact sensors: Do not require physical contact
  1. The last one provides several advantages over contacting devices including the no risk of damaging a fragile part because of contact with the measurement probe, and parts can be measured in highly dynamic processes and environments as they are manufactured.

### 1.3.1 Capacitive

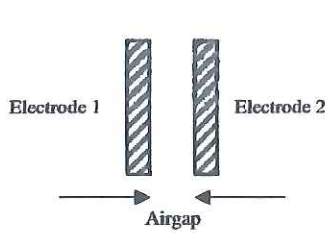
Capacitive effect is the ability of a pair of electrodes to hold an electric charge and can directly sense a variety of things—motion, chemical composition, electric field—and, indirectly, sense many other variables which can be converted into motion or dielectric constant, such as pressure, acceleration, fluid level, and fluid composition. The capacitive sensors are non-contact devices that are built with conductive sensing electrodes in a dielectric, with excitation voltages.

Basically there are three different applications for these devices [8]:

1. To detect material properties
2. To sense motion or position
3. To detect proximity

The simplest model of this is two metal plates with an air gap between them (Fig 1-4). When using capacitive sensors, the sensor is one of the conductive plates and the target is the other. Capacitive sensors measure changes in the capacitance between the sensor and

the target by creating an alternating electric field between the sensor and the target and monitoring changes in the electric field.



$$C = \iint \epsilon_r \epsilon_0 \frac{dxdy}{z(x, y)}$$

Where:

$\epsilon_r$  is the media relative dielectric constant (for air, it is very close to 1).

$\epsilon_0$  is the dielectric constant of vacuum (8.85E-12 F/m)

$Z(x,y)$  is the gap distance between the electrodes.

Fig 1-4. Two parallel plates. Simplest capacitor array

### 1.3.2 Magnetism

The space surrounding a magnet is said to contain a magnetic field. The physical force exerted by a magnet can be described as lines of flux originating at the north pole of a magnet and terminating at its south pole. As a result, lines of flux are said to have a specific direction. Moreover, because there are no magnetic charges, magnetic field lines can never have a beginning or an end. Magnetic field lines always form closed loops. The concept of flux density is used to describe the intensity of the magnetic field at a particular point in space. Flux density is used as the measure of magnetic field. Units of flux density include teslas and webers/meter<sup>2</sup>. [10], One of the current sensing devices that use the magnetism is the hall sensor. When a current-carrying conductor is placed into a magnetic field, a voltage will be generated perpendicular to both the current and the field. This principle is known as the Hall effect.

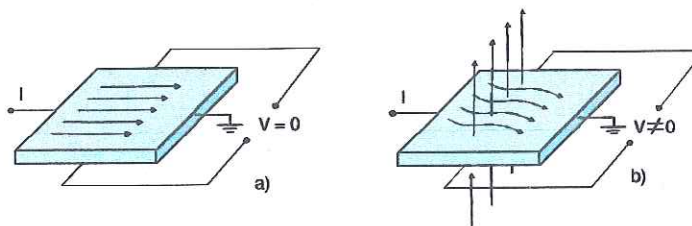


Fig 1-5. Hall element. a) Current passes through. The output connections are perpendicular to direction of current. Current distribution is uniform when magnetic field is not present. b) When a perpendicular magnetic field is present, a Lorentz force is exerted on the current. This force disturbs the current distribution, resulting in a potential difference (voltage) across the output.

### 1.3.3 Inductance

Is the ability of a varying magnetic field to induce electric current in a wire. Electric current is generated as long as the magnetic field changes. A stationary field produces no current. Faraday's law of induction says that the induced voltage, or electromotive force (e.m.f.), is equal to the rate at which the magnetic flux through the circuit changes. An inductor is a passive circuit element that resists changes in current. There is a voltage across the inductor whenever the current changes which is to say that whenever an external circuit tries to cause more current to flow, it must provide a voltage in order to overcome the voltage that arises in the inductor [7, 4]. The equation governing its behavior is:

$$V = -L \frac{\partial I}{\partial t} \quad \text{where } L \text{ is the inductance in units of henrys. The minus sign indicates that the voltage (V) opposes the change in current (I).}$$

Unlike the capacitive sensors, inductive sensors are not affected by material in the probe/target gap. Inductive sensors, also known as eddy current sensors, are non-contact devices and they are well adapted to hostile environments that may appear in the gap. Inductive sensors are sensitive to the type of target material.

### 1.3.4 Resistance

The electrical resistance is the opposition of a body to allow electrical current flows through the same body.

$$R = \rho \frac{l}{a} = \frac{m}{n \cdot e^2 \cdot \tau} \frac{l}{a}$$

Where (l) is the length and (a) is the area or cross section of the conductor;  $\rho$  is the resistivity of the material. The resistivity of a material can be expressed through mean time between collisions  $\tau$ , the electronic charge e, the mass of electron m, and a number of conduction electrons per unit volume n. There are several sensing devices under the resistance effect; two of them are the RTD and strain gauges.



- **RTD:** Are sensors that changes resistance value as its temperature changes.
- **Strain gauges:** The strain gauges are connected in a four-arm Wheatstone bridge configuration, which acts as an adding and subtracting electrical network and allows for compensation of temperature effects as well as cancellation of signals caused by extraneous forces. The applied input is translated into a voltage by the resistance change in the strain gages, which are intimately bonded to the transducer structure. The amount of change in resistance indicates the magnitude of deformation in the transducer structure and hence the load that is applied [7].

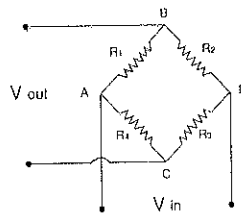


Fig 1-6. Wheatstone bridge configuration for strain gages sensing element.

### 1.3.5 Piezoelectric

The piezoelectric effect is the generation of electric charge by a crystalline material upon subjecting it to mechanical stress. The effect exists in natural crystals, such as quartz (chemical formula  $\text{SiO}_2$ ), and poled (artificially polarized) man-made ceramics and some polymers, such as polyvinylidene fluoride. It is said that piezoelectric materials possess ferroelectric properties.

The brothers Pierre and Jacques Curie discovered the piezoelectric effect in 1880. They found that some crystalline materials were generating an electrical polarization when subjected to a mechanical load along some crystal directions.

The main advantages of piezoelectric sensors are:

1. Wide measuring range (span to threshold ratio up to 108)
2. High rigidity (high natural frequency)
3. High linearity between output signal and applied load
4. High reproducibility and stability of the properties (when single crystals are used)

5. Wide operating temperature range
6. Insensitive to electric and magnetic fields

The piezoelectric effect is a reversible physical phenomenon. That means that applying voltage across the crystal produces mechanical strain. By placing several electrodes on the crystal, it is possible to use one pair of electrodes to deliver voltage to the crystal and the other pair of electrodes to pick up charge resulting from developed strain [4, 7].

### 1.3.6 Optical

Optical components help to manipulate light in many ways by using an optical element. This manipulation involves changing of direction (reflection) or by using selective blocking of certain wavelength (filtering) [4]. Light has an electromagnetic nature and is a quantum-mechanical phenomena; it comes in discrete particles called photons.

In optics, there are two fields of study:

- Radiometry studies the measurement of electromagnetic radiation, including ultraviolet, visible light and the infrared.
- Photometry is the measurement of light, which is defined as electromagnetic radiation that is detectable by the human eye.

The only real difference between radiometry and photometry is that radiometry includes the entire optical radiation spectrum, while photometry is limited to the visible spectrum as defined by the response of the eye.

### 1.3.7 Resonance

Is the tendency of a system to oscillate at maximum amplitude at certain frequencies. The possibility of resonance always exists wherever there is periodic motion, movement that is repeated at regular intervals called periods, and/or harmonic motion, the repeated movement of a particle about a position of equilibrium or balance. When the forcing function's frequency matches the natural frequency of an object it will begin to resonate. Resonance requires 3 basic conditions:

- An object with a natural frequency: An object's natural frequency is the frequency it tends to oscillate at when disturbed. The oscillation can be a mechanical

vibration or in an electronic circuit the oscillation is a variable voltage or current. An object can have more than one natural frequency. These are called harmonics.

- A forcing function at the same frequency as the natural frequency: In mechanical systems the forcing function is a variable force. In electronic circuits it arises from a variable electric field.
- Lack of damping or energy loss: Damping is a means of removing electrical or mechanical energy by converting it to another type of energy as friction or heat.

## Chapter 2. Capacitive sensors

### 2.1 Introduction

In general, any capacitive sensor is quite better than those contact devices and actually may be also cheaper; however there are some technical limitations due to the nature of the sensing element:

- 1) Dirty environment of spraying fluids, dust, metal chips.
- 2) For non uniform thickness of the dielectric layer, the calibration of the sensor becomes complex and tedious.

Besides those technical challenges, capacitive technology is quite used for most of the sensors devices available on the market, so for any newer design the price becomes the critical factor to succeed the design.

In the following pages, there will be presented more understanding theory and information behind the design and characteristics of a capacitive sensor device; and available product portfolio for this technology based on the current devices available on the market.

### 2.1.1 Operational principle

Capacitive effect is the ability of a pair of electrodes to hold an electric charge which is widely used for many sensing devices. Capacitive sensors are non-contact devices [4] used for precision measurement of a conductive target's position or a nonconductive material's thickness or density. When used with conductive targets they are not affected by changes in the target material; all conductors look the same to a capacitive sensor. Capacitive sensors sense the surface of the conductive target, so the thickness of the material is not an issue; even thin plating is a good target. Technically speaking, the capacitance is directly proportional to the surface area of the objects and the dielectric constant of the material between them, and inversely proportional to the distance between them. In typical capacitive sensing applications, the probe or sensor is one of the conductive objects; the target object is the other. The sizes of the sensor and the target are assumed to be constant as is the material between them. Therefore, any change in capacitance is a result of a change in the distance between the probe and the target. Capacitive sensors can directly sense a variety of motion, chemical composition and electric field and, indirectly, sense many other variables which can be converted into motion or dielectric constant, such as pressure, acceleration, fluid level, and fluid composition [8]. They are built with conductive sensing electrodes in a dielectric, with excitation voltages and detection circuits which turn a capacitance variation into a voltage, frequency, or pulse width variation.

### 2.1.2 Sensing element

There is not such a step by step list to design the best capacitive sensing element; however we can pronounce a general design process:

1. Design electrode plates to measure the desired variable. Maximize capacitance with large-area, close-spaced plates
2. Surround this sensor with appropriate guard or shield electrodes to handle stray capacitance and crosstalk from other circuits

3. Calculate sensor capacitance, stray capacitance and output signal swing
4. Specify transfer function
5. Choose an excitation frequency high enough for low noise. As excitation frequency increases, external and circuit-generated noise decreases
6. Design circuit to meet accuracy specifications and provide immunity to environmental challenges

The calculation of the capacitance for two conductive electrodes can be analytically calculated by the next expression:

$$C = \iint \epsilon_r \epsilon_0 \frac{dx dy}{z(x, y)}$$

The capacitance is affected by three things: the sizes of the probe and target surfaces, the distance between them, and the material that is in the gap; so any combination of these factors may conduct different sensing element designs however all of them come from the original definition –two parallel electrodes with a dielectric media in between–.(Fig 2-1).

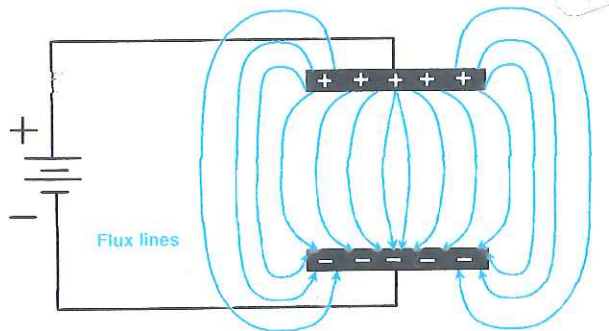


Fig 2-1. Electric field between two charged conducting plates

Computational simulation can be used to calculate the capacitance for symmetrical and non-symmetrical electrode's shape. Several simulation softwares available on the market based on FEA integrate pre-processor (drawing and boundary conditions), solver and

post-processor (visualization plots) that can provide accurate results and shorten the design stage (Fig 2-2).

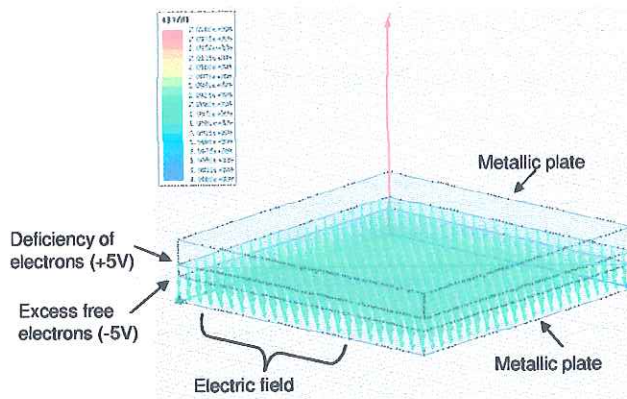


Fig 2-2. Electric field by Computational Simulation (ANSOFT) for symmetrical electrode's shape

Based on the application, the electrodes may have three different geometries: Round, Planar and Combined.

- Round Geometry

Depending on the application, this design may be suitable to use round electrodes such as electronic key pads or metallic fuel tanks.

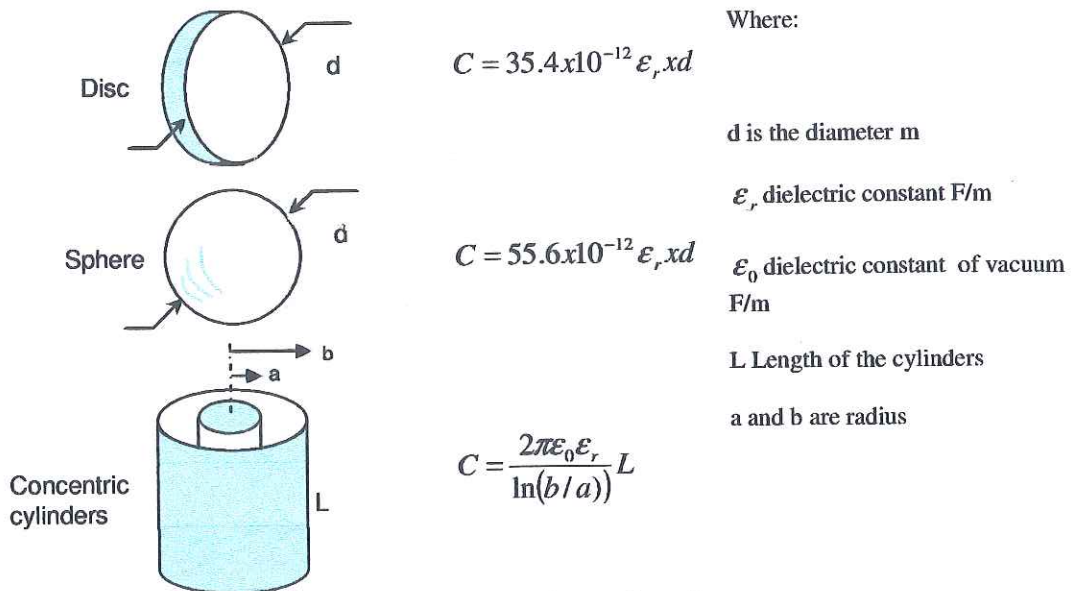


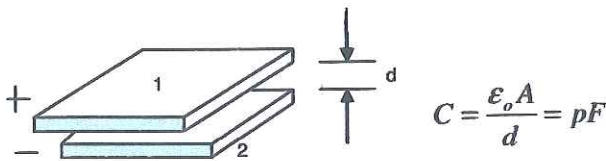
Fig 2-3. Round capacitor configurations

- Planar Geometry

This is one of the most used configurations for a capacitive device used due to the simplicity of the design. It uses two parallel conductive plates (flat electrodes) separated by a non conductive region called dielectric (Fig 2-4). Both electrodes contain equal and opposite charges.

The versatility and simplicity of this design can be used to make different configurations:

- Overlapping parallel plates with different areas
- Coplanar plates with X-Y displacement
- Coplanar plates with different areas front of a 3<sup>rd</sup> electrode electrically grounded

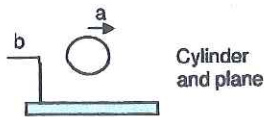


Where:

A is the plate area  $m^2$   
d is the distance between plates m  
 $\epsilon_0$  dielectric constant F/m

Fig 2-4. Planar capacitor configurations

- Combined geometry



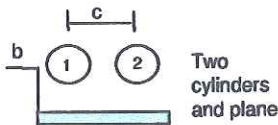
$$C = \frac{2\pi\epsilon_0\epsilon_r L}{\ln\left[\frac{b + \sqrt{b^2 - a^2}}{a}\right]}$$

$$= \frac{2\pi\epsilon_0\epsilon_r L}{a \cosh(b/a)}$$

Where:

b is the separation between two conductors m

$\epsilon_r$  dielectric constant F/m



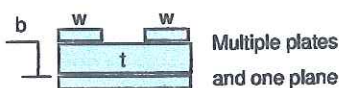
$$C_m \approx \frac{\pi\epsilon_0\epsilon_r L \cdot \ln\left[1 + \frac{2b}{c}\right]}{\left[\ln\left(\frac{2b}{a}\right)\right]^2}$$

$\epsilon_0$  dielectric constant of vacuum F/m

L Length of the cylinder(s)

a and b are radius

$\epsilon_{r(eff)}$  effective dielectric constant



$$C_m \approx \frac{\pi\epsilon_0\epsilon_{r(eff)} L}{\left[\ln\left(\frac{\pi(c-w)}{w+t} + 1\right)\right]}$$

W is the width of the strips

C separation between electrodes

Fig 2-5. Combined capacitor configurations

### 2.1.13 Technical requirements

Some advantages of the capacitive technology over others are:

- Higher resolution.
- Not sensitive to material changes. Capacitive sensors respond equally to all conductors.
- Less expensive and much smaller than laser interferometers.

However, some observed disadvantages of this technology are related to reduce its use under the following environments:

- Dirty or wet environments
- Large gap between sensor and target is required

Considerations must be taken to conduct a good capacitive design with maximum sensitivity [4].

- The target size is a primary consideration when selecting a probe for a specific application. When the sensing electric field is focused by guarding, it creates a slightly conical field that is a projection of the sensing area. The minimum target diameter for standard calibration is 30% of the diameter of the sensing area. The further the probe is from the target, the larger the minimum target size.
- The range in which a probe is useful is a function of the size of the sensing area. The greater the area, the larger the range. The driver electronics are designed for a certain amount of capacitance at the probe. Therefore, a smaller probe must be considerably closer to the target to achieve the desired amount of capacitance. The electronics are adjustable during calibration but there is a limit to the range of adjustment.
- Frequently, a target is measured simultaneously by multiple probes. Because the system measures a changing electric field, the excitation voltage for each probe must be synchronized or the probes would interfere with each other. If they were not synchronized, one probe would be trying to increase the electric field while another was trying to decrease it thereby giving a false reading.
- The sensing electric field is seeking a conductive surface. Provided that the target is a conductor, capacitive sensors are not affected by the specific target material.



Because the sensing electric field stops at the surface of the conductor, target thickness does not affect the measurement.

- For non-conductive target materials like plastic have a different dielectric constant than air. The dielectric constant determines how a non-conductive material affects capacitance between two conductors. When a non-conductor is inserted between the probe and a stationary reference target, the sensing field passes through the material to the grounded target. The presence of the non-conductive material changes the dielectric and therefore changes the capacitance. The capacitance will change in relationship to the thickness or density of the material.

## 2.2 Applications/Current devices

The capacitive sensors have a wide variety of uses [8]:

### Proximity sensing

- Personnel detection. Safety shutoff when machine operator is too close
- Light switch. A capacitive proximity sensor with 1m range can be built into a light switch for residential use
- Vehicle detection. Traffic lights use inductive loops for vehicle detection. Capacitive detectors can also do the job, with better response to slow-moving vehicles

### Measurement

- Flow. Many types of flow meters convert flow in pressure or displacement, using an orifice for volume flow or Coriolis Effect force for mass flow [Jones, 1985]. Capacitive sensors can then measure the displacement directly, or pressure can be converted to a displacement with a diaphragm.
- Pressure. With gases or compressible solids a pressure change may be measured directly as dielectric constant change or a loss tangent change.

- Liquid level. Capacitive liquid level detectors sense the liquid level in a reservoir by measuring changes in capacitance between parallel conducting plates which are immersed in the liquid, or applied to the outside of a non-conducting tank.
- Spacing. If a metal object is near a capacitor electrode, the coupling between the two is a very sensitive way to measure spacing.
- Scanned multiplate sensor. The single plate spacing measurement concept above can be extended to contour measurement by using many plates, each separately addressed. Both conductive and dielectric surfaces can be measured.
- Thickness measurement. Two plates in contact with an insulator will measure the thickness if the dielectric constant is known or the dielectric constant if the thickness is known.
- Ice detector. Airplane wing icing can be detected using insulated metal strips in wing leading edges.
- Shaft angle or linear position. Capacitive sensors can measure angle or position with a multiplate scheme giving high accuracy and digital output or with analog output with less absolute accuracy but simple circuitry.
- Balances. A spring scale can be designed with very low displacement using a capacitive sensor to measure plate spacing. A similar technique can measure mass, tilt, gravity or acceleration.
- Accelerometers. Analog Devices has introduced integrated accelerometer ICs with a sensitivity of 1.5g. With this sensitivity, the device can be used as an altimeter.

#### Switches

- Lamp dimmer. The standard metal-plate soft-touch lamp dimmer uses 60 Hz excitation and senses the capacitance of the human body to ground.
- Keyswitch. Capacitive keyswitches use the shielding effect of the nearby finger or a moving conductive plunger to interrupt the coupling between two small plates.
- Limit switch. Limit switches can detect the proximity of a metal machine component as an increase in capacitance, or the proximity of a plastic component by virtue of its increased dielectric constant over air.

## Communications

- Wireless datacomm. Data are capacitively coupled across a short gap in a device which replaces the optical isolator. RF in the near field can be sensed by a receiver with a capacitive plate antenna.

## Computer graphic input

- X-Y tablet. Capacitive graphic input tablets of different sizes can replace the computer mouse as an x-y coordinate input device. Finger-touch-sensitive, z-axis-sensitive and stylus-activated devices are available.

## PART III. THEORY

### Chapter 3. The High Pressure Sensor

#### 3.1 Introduction

The High Pressure Sensor (HPS) is a project belong Delphi's product portfolio focused to investigate and implement a reliable technological solution for a low cost alternative to the current crowded market of the pressure sensors that can be installed at the Delphi's Gasoline Direct Injection (GDI).

This sensor must meet several technical requirements and most important, the final packaging needs to be versatile in such a way that the same sensor's design can be used to fit different applications –pressure ranges from low to high- by making minor modifications that will not impact the functionality of the sensing element. Some of the current technologies for pressure measurement sensors include piezoresistive technology -thick film and thin film which involve, building a strain gage on the top surface of a sensing membrane- and MEMS. There are devices that use the same capacitive principle with a flexible sensing element, however their design is complex and the membrane is not compatible with the media.

##### 3.1.1 Operational principle

Based on the capacitive technology of two parallel electrodes separated by a dielectric media; the HPS provides an electrical output signal according to a variation of an inlet pressure from a pressurized system (Fig 3-1).

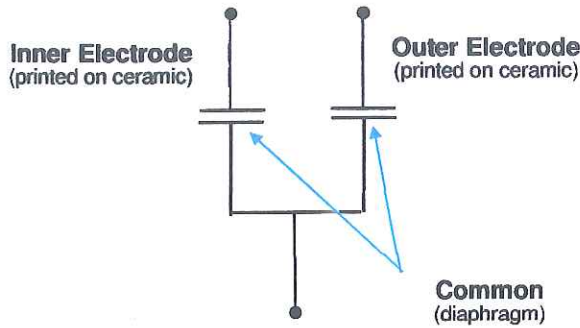


Fig 3-1. Electric capacitance configuration

The sensing element of the HPS is basically formed by three main components:

- a) Deflective conductive diaphragm
- b) Two concentric electrodes printed onto a rigid PCB
- c) Gap

These three components create a variable capacitor whose capacitance varies according to the change in the differential arrangement of the traces (electrodes printed onto PCB). The two concentric traces, -one surrounds the other- are electrically connected to an electronic circuitry and are separated from the deflective diaphragm by using a shim (or step fabricated on top of diaphragm) in order to create an empty cavity. The outer electrode remains in intimate contact with the diaphragm and its characteristics remains constant. This electrode can be considered as reference capacitor due to not change of capacitance (Fig 3-2).

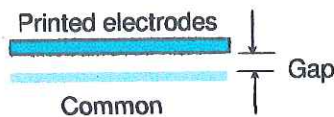


Fig 3-2. Principle of operation. Capacitance at zero deflection.

As soon as pressure rises, the diaphragm deflects in a centered dome shape that only affects the capacitance in the second capacitor created by the inner electrode (Fig 3-3).

This shift in capacitance is proportional to the change in gap between the inner electrode and the diaphragm.



Fig 3-3. Principle of operation. Capacitance at diaphragm deflected

With changes in pressure results in change in capacitance of the centered capacitor, with possible effect in the outer capacitor (will depend of the flatness of it). Finally, the pressure signal generating circuit is responsive to variations in the capacitance of the first and second capacitors, preferably measured in a differential mode, to generate a pressure signal indicative of the fluid pressure.

### 3.1.2 Sensing element

As previously mentioned, the sensing element of the HPS is based on the differential capacitance between two concentric electrodes printed on a ceramic board and a step component on top of a flat diaphragm. The design rules and specific information of each of these components will be further explained on Part IV and V.

#### a) Deflective conductive diaphragm

- Deflects against pressure
- Withstand high stress ratio due to reaction loads at clamped edges
- Provides electrical connection (common) for both electrodes

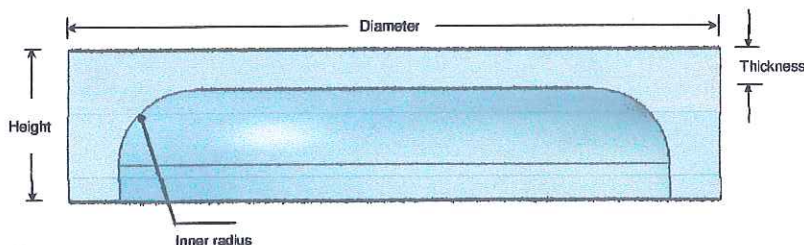


Fig 3-4. Cross section view of diaphragm

b) Two concentric electrodes printed onto a rigid PCB

- Provides the parallel capacitor arrangement
- Shields against parasitic capacitances
- Places the electronic components

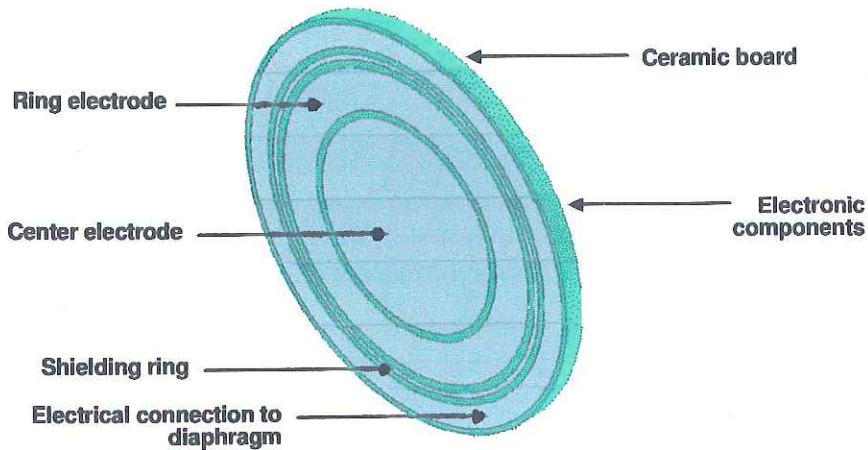


Fig 3-5. Electrodes arrangement on printing circuit board (PCB)

c) Gap

- Provides the necessary distance to allow the deflection of the diaphragm and reduce the risk of electric short
- Allows change in capacitance
- Provides electrical contact (common) between diaphragm and electrodes

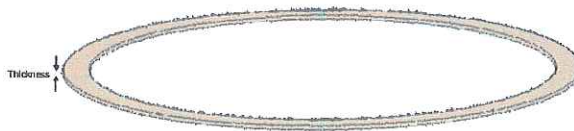


Fig 3-6. Step ring provides the airgap (thickness)

In addition to the electrode traces, the substrate (PCB) is formed by several other layers in order to guarantee the correct output signal condition delivered (Fig 3-7).

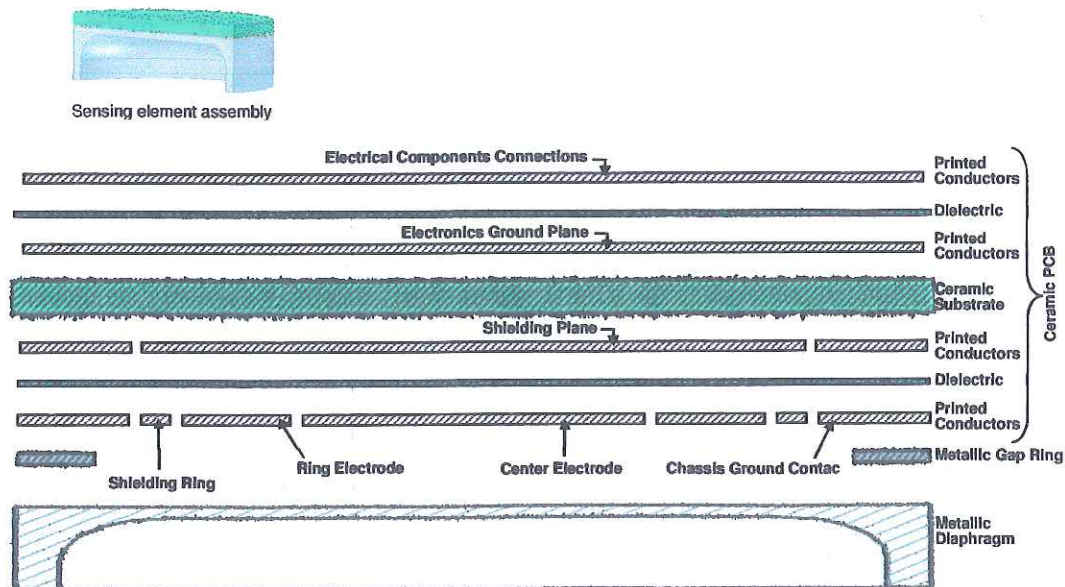


Fig 3-7. Sensing element assembly

The complete sensing element assembly also encloses electronic components that are electrically connected to the electrodes' circuit, through vias formed through the insulating substrate. The electronic circuit is located on the other side of the substrate.

### 3.1.3 Technical requirements

As previously mentioned, the HPS was pointed to be installed at the Delphi's GDI system; so the technical requirements come from the Diesel Common Rail specifications.

Before going on board with technical data, as prior art the Gasoline Direct Injection (GDI) precisely manages fuel spray into an engine and allows for a higher compression ratio, resulting in improved engine performance and reduced fuel consumption.



Mercedes-Benz was the first automaker to use gasoline fuel injection - direct injection at that - with the 1955 Mercedes Benz 300SL. Adapted by Bosch from aircraft applications, this mechanical system placed a fuel injector inside each of the spark-plug bores in the cylinder wall. This first automotive application of GDI bestowed the SL's 6-cylinder with more than twice the power of the carbureted production 6 (240 hp, up from 115 hp). It also gave the engine 10 percent better fuel consumption than the carbureted engine that ran and won Le Mans in 1952. Fuel injection ensured the 300SL was not only one of the most revolutionary cars of its era, but also one of the fastest [11].

Except on operating pressure, proof pressure and burst pressure, the rest of the technical requirements are similar for both pressure sensor design (500 and 3000 PSI). The following Table 1 shows technical requirements for 3000 PSI.

		Unit	Target
Technical Points of Difference	Accuracy: full scale output deviations	% F.S.	$\pm 2.0$
	Time response	ms	2
	Hermetic	cc/sec	1.00E-07
	Operating pressure range (0.5 to 4.5V output)	bar	200
	Proof pressure (maintains constant 4.5V output)	bar	260
	Burst pressure	bar	362
	Operating Temperature	$^{\circ}\text{C}$	-40 to 130
	Mechanical life durability: 10M pressure cycles	cycles	
Relative price points	Price	\$	<b>Not shown</b>

Table 1. Technical requirements for HPS 3000 PSI

### 4.1 Introduction

The theory behind the design and predicted performance of the diaphragm is theoretical well known if it is calculated as flat circular plate clamped over the edges and assumed uniform pressure over surface. It is not pretended to develop a rigorous mathematical partial differential equation, however it will be presented an explanation of the "Thin plate theory" that is actually desirable to explain and provide the insight of the stress-deflection behavior for the proposed diaphragm design. The "Thick plate" theory will be also presented; however equation substitution-demonstration is not intended to demonstrate as prior theory.

- Thin plate or small deflection theory.  
Where: Deflection  $\leq 0.2$  Thickness
- Thick plate or large deflection theory.  
Where: Deflection  $\leq 3$  Thickness

### 4.2 Thin plate theory

#### 4.2.1 Small deflection theory

Small deflection theory is based on the Kirchoff-Love hypotheses:

1. The diaphragm material is flat and uniform thickness.
2. The material is elastic, homogenous, isotropic and continuous
3. The elastic limit of the material is not exceeded
4. Deformation is due to bending, the neutral axis of the diaphragm experiences no stress

5. The bending deflections are small compared to the thickness of the plate. The slope of the deflected plate is also small; hence the square of the deflection is small
6. Pressure is applied normally to the plane of diaphragm
7. Plane sections originally normal to the surface are presumed to be normal after bending. Hence shearing strains  $\gamma_{rz}$  and  $\gamma_{\theta z}$  are negligible. The stresses  $\sigma_z$  are small and can be neglected.
8. The deflections of the plate are due to the displacements of points in the middle surface of the plate in a direction normal to the non-deflected middle surface.

As a consequence of condition 7, plane stress is said to be in effect [1]

$$\epsilon_x = \frac{z}{r_x} \Rightarrow r_x = \frac{z}{\epsilon_x} \quad \epsilon_y = \frac{z}{r_y} \Rightarrow r_y = \frac{z}{\epsilon_y} \quad (4.1)$$

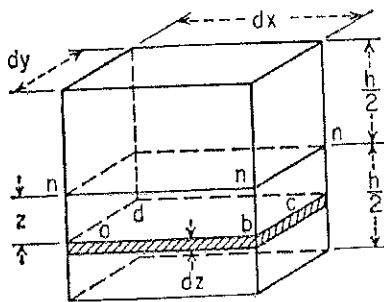


Fig 4-1. Graphical representation of the unit elongations in the x and y directions of an element lamina 'abcd' at a distance z from the neutral surface

Using the Hooke's law, the corresponding stresses in the lamina 'abcd' are:

$$\sigma_x = \frac{Ez}{1-\nu^2} \left( \frac{1}{r_x} + \nu \frac{1}{r_y} \right) \quad \sigma_y = \frac{Ez}{1-\nu^2} \left( \frac{1}{r_y} + \nu \frac{1}{r_x} \right) \quad (4.2)$$

so that for cylindrical coordinates mechanical stress ( $\sigma_z$ ) and shear stress ( $\tau_{rz}$ ,  $\tau_{\theta z}$ ) are all zero and the stress-strain relationships become

$$\begin{aligned} \varepsilon_r &= \frac{1}{E}(\sigma_r - \nu\sigma_\theta) & \sigma_r &= \frac{E}{1-\nu^2}(\varepsilon_r + \nu\varepsilon_\theta) \\ \varepsilon_\theta &= \frac{1}{E}(\sigma_\theta - \nu\sigma_r) & \sigma_\theta &= \frac{E}{1-\nu^2}(\varepsilon_\theta + \nu\varepsilon_r) \end{aligned} \quad (4.3)$$

The general equations for bending of plates in polar coordinates, the  $r$  and  $\theta$  coordinates are taken from the relation between the polar and Cartesian coordinates:

$$r^2 = x^2 + y^2 \quad \theta = \arctan \frac{y}{x} \quad (4.4)$$

From which it follows that:

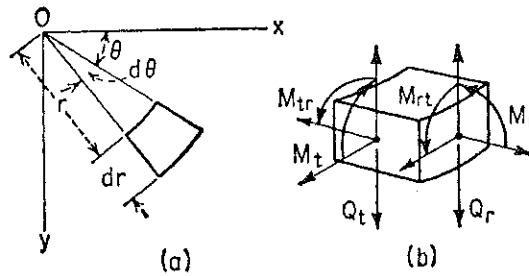


Fig 4-2. Relation between Cartesian and polar coordinates.

$$\begin{aligned} \frac{\partial r}{\partial x} &= \frac{x}{r} = \cos \theta & \frac{\partial r}{\partial y} &= \frac{y}{r} = \sin \theta \\ \frac{\partial \theta}{\partial x} &= -\frac{y}{r^2} = -\frac{\sin \theta}{r} & \frac{\partial \theta}{\partial y} &= \frac{x}{r^2} = \frac{\cos \theta}{r} \end{aligned} \quad (4.5)$$

The slope of the deflection surface of a plate in the  $x$  direction is:

$$\begin{aligned} \frac{\partial w}{\partial x} &= \frac{\partial w}{\partial r} \frac{\partial r}{\partial x} + \frac{\partial w}{\partial \theta} \frac{\partial \theta}{\partial x} = \frac{\partial w}{\partial r} \cos \theta - \frac{1}{r} \frac{\partial w}{\partial \theta} \sin \theta \\ \frac{\partial w}{\partial y} &= \frac{\partial w}{\partial r} \frac{\partial r}{\partial y} + \frac{\partial w}{\partial \theta} \frac{\partial \theta}{\partial y} = \frac{\partial w}{\partial r} \sin \theta + \frac{1}{r} \frac{\partial w}{\partial \theta} \cos \theta \end{aligned} \quad (4.6)$$

To obtain the expression for curvature in polar coordinates the second derivatives are required:

$$\begin{aligned}\frac{\partial^2 w}{\partial x^2} &= \frac{\partial^2 w}{\partial r^2} \cos^2 \theta - 2 \frac{\partial^2 w}{\partial \theta \partial r} \frac{\sin \theta \cos \theta}{r} + \frac{\partial w}{\partial r} \frac{\sin^2 \theta}{r} + 2 \frac{\partial w}{\partial \theta} \frac{\sin \theta \cos \theta}{r^2} + \frac{\partial^2 w}{\partial \theta^2} \frac{\sin^2 \theta}{r^2} \\ \frac{\partial^2 w}{\partial y^2} &= \frac{\partial^2 w}{\partial r^2} \sin^2 \theta + 2 \frac{\partial^2 w}{\partial \theta \partial r} \frac{\sin \theta \cos \theta}{r} + \frac{\partial w}{\partial r} \frac{\cos^2 \theta}{r} - 2 \frac{\partial w}{\partial \theta} \frac{\sin \theta \cos \theta}{r^2} + \frac{\partial^2 w}{\partial \theta^2} \frac{\cos^2 \theta}{r^2}\end{aligned}\quad (4.7)$$

With this transformation of coordinates we obtain

$$\Delta w = \frac{\partial^2 w}{\partial x^2} + \frac{\partial^2 w}{\partial y^2} = \frac{\partial^2 w}{\partial r^2} + \frac{1}{r} \frac{\partial w}{\partial r} + \frac{1}{r^2} \frac{\partial^2 w}{\partial \theta^2} \quad (4.8)$$

Repeating this operation twice, the differential equation of equilibrium for deflection surface

$$\frac{\partial^4 w}{\partial x^4} + 2 \frac{\partial^4 w}{\partial x^2 \partial y^2} + \frac{\partial^4 w}{\partial y^4} = \Delta \Delta w = \frac{P}{D} \quad (4.9)$$

Transforms in polar coordinates to the following form:

$$\Delta \Delta w = \frac{P}{D} = \left( \frac{\partial^2}{\partial r^2} + \frac{1}{r} \frac{\partial}{\partial r} + \frac{1}{r^2} \frac{\partial^2}{\partial \theta^2} \right) \left( \frac{\partial^2 w}{\partial r^2} + \frac{1}{r} \frac{\partial w}{\partial r} + \frac{1}{r^2} \frac{\partial^2 w}{\partial \theta^2} \right) \quad (4.10)$$

When the load is symmetrically distributed with respect to the center of the plate, the deflection  $w$  is independent of  $\theta$ , and coincides with equation of symmetrically loaded circular plates:

$$\frac{1}{r} \frac{d}{dr} \left\{ r \frac{d}{dr} \left[ \frac{1}{r} \frac{d}{dr} \left( r \frac{dw}{dr} \right) \right] \right\} = \frac{P}{D} \quad (4.11)$$

Most deflective diaphragms are considered to have clamped boundary conditions, that is

$$w(r=\text{edge}) = 0 \quad \left. \frac{\partial w}{\partial r} \right|_{r=\text{edge}=0} = 0 \quad (4.12)$$

from symmetry arguments, the following additional boundary condition is expected:

$$\left. \frac{\partial w}{\partial \theta} \right|_{r=\text{center}} = 0 \quad (4.13)$$

Finally, the amount of radial stretch,  $u$ , of the diaphragm at the edge is zero. As a consequence the circumferential strain in the middle of the thickness of the diaphragm is also zero. Solving this equation for azimuthal symmetry and clamped boundary conditions [1] such that:

$$w(r) = \frac{Pa^4}{64D} \left( 1 - \left( \frac{r}{a} \right)^2 \right) \quad (4.14)$$

The radial strain is:  $\epsilon_r = -\frac{z}{\rho_r}$       The circumferential strain is:  $\epsilon_\theta = -\frac{z}{r} \frac{dw}{dr}$       (4.15)

where  $z$  is the distance from the center of the diaphragm and  $\rho_r$  is the radius of curvature of the deflected diaphragm. At the top of the diaphragm  $z = -\frac{h}{2}$ . Also, for

small deflections,  $\rho_r = \frac{\partial^2 w}{\partial r^2}$ . Hence the strains become:

$$\epsilon_r = \frac{Pa^2 h}{32D} \left( 3 \left( \frac{r}{a} \right)^2 - 1 \right) \quad \epsilon_\theta = \frac{Pa^2 h}{32D} \left( \left( \frac{r}{a} \right)^2 - 1 \right) \quad (4.16)$$

In these equations, negative strain is compressive, while positive strain is tensile. Normalized strains for the top surface of a thin plate are plotted in Figure 4-3.

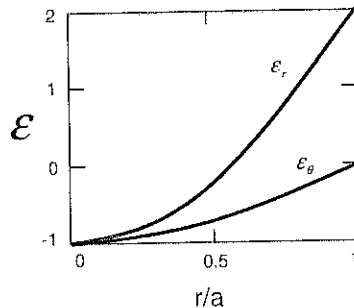


Fig 4-3. Normalized strain ( $Pa^2 h / 32D$ ) vs. normalized position for thin plate.

The radial strain is negative in the center of the diaphragm and positive on the edges, whereas circumferential strain is always negative.

#### 4.3 Large deflection theory

In order to obtain a satisfactory solution for large deflections of a uniformly loaded circular plate with a clamped edge, it is necessary to solve the equilibrium equation based on Timoshenko's [1] and Szilard's [15] rationale for a deflected circular plate.

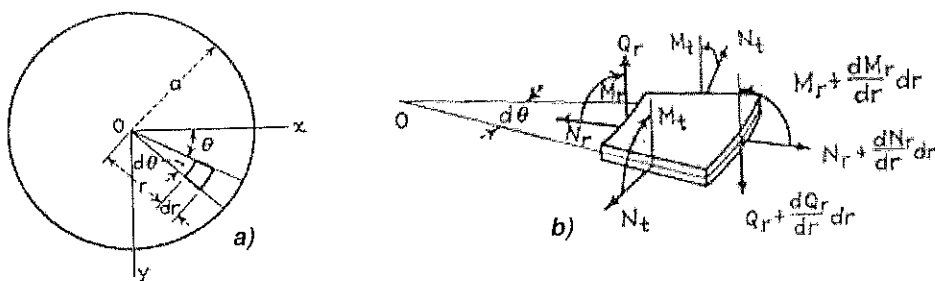


Fig 4-4. a) Tensile forces per unit length  $N$ . b) Projection in radial direction of forces  $N$  and moments  $M$  uniformly distributed along the edge of the plate

The stored strain energy is first separated into two parts:

- a) The energy of bending  $V_1$
- b) The energy due to the stretching of the middle plane  $V_2$

Based on the small deflection equation (4.14) and

$$V_1 = \frac{32\pi w_0^2 D}{3a^2} \quad (4.17)$$

The energy due to the stretching of the middle plane is derived by assuming that the radial displacement "u" matches the clamped boundary conditions as well as the center position of the plate

$$u = r(a-r)(C_1 + C_2 r + C_3 r^2 + \dots) \quad (4.18)$$

If the first two terms in (4.18) are considered constants and can be determined by taking the total energy of the plate for an equilibrium position in a minimum. Therefore, both constants can be determined

$$\begin{aligned} C_1 &= 1.185 \frac{w_0^2}{a^3} \\ C_2 &= -1.75 \frac{w_0^2}{a^4} \end{aligned} \quad (4.19)$$

and  $V_2$  can be derived as

$$V_2 = 2.59\pi D \frac{w_0^4}{a^2 h^2} \quad (4.20)$$

The total strain energy is the combination of  $V_1$  and  $V_2$ . Based on the principle of virtual displacement

$$\frac{d(V_1 + V_2)}{dw_0} \delta w_0 = 2\pi q \delta w_0 \int_0^a \left(1 - \frac{r^2}{a^2}\right)^2 r dr \quad (4.21)$$

The maximum deflection is derived as

$$w_0 = \frac{qa^2}{64D} \frac{1}{\left(1 + 0.488 \frac{w_0^2}{h^2}\right)} \quad (4.22)$$

Therefore, (4.22) can be used to calculate the maximum deflection if the loading is given. The deflection can then be derived by using (4.14). The displacement can be calculated by (4.18), and the stress and strain at any point of the diaphragm can be solved by using (4.23).



$$\begin{aligned}\varepsilon_{xx} &= \frac{\partial u}{\partial x} + \frac{1}{2} \left( \frac{\partial w}{\partial x} \right)^2 \\ \varepsilon_{yy} &= \frac{\partial u}{\partial y} + \frac{1}{2} \left( \frac{\partial w}{\partial y} \right)^2 \\ \varepsilon_{xy} &= \frac{1}{2} \left( \frac{\partial u}{\partial y} + \frac{\partial u}{\partial x} \right) + \left( \frac{\partial w}{\partial x} \frac{\partial w}{\partial y} \right)\end{aligned}\tag{4.23}$$

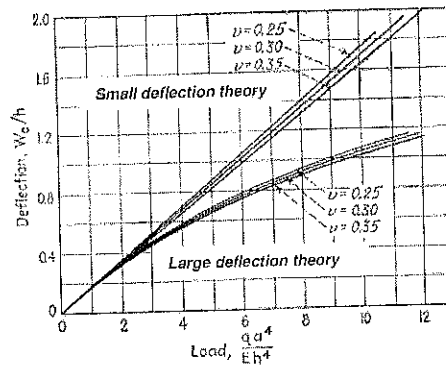


Figure 4-5. Corresponding stress ratio for small and large deflection theories.

#### 4.4 Dynamic characteristics

In the context of this work, dynamic behavior refers to the response of a diaphragm to natural frequencies due to free vibration. The complete solution of the problem of free vibration of any system would require the determination of all the natural frequencies and of the mode shape associated with each. In practice, it often is necessary to know only a few of the natural frequencies, and sometimes only one. Usually the lowest frequencies are the most important. The exact mode shape is of secondary importance in many problems.

Degrees of freedom [15]: In physical systems, all elastic members have mass, and all masses have some elasticity; thus, all real systems have distributed parameters. In making an analysis, it is often assumed that real systems have their parameters lumped. Systems with distributed parameters are characterized by having an infinite number of degrees-of-

freedom. For example, if an initially straight beam deflects laterally, it may be necessary to give the deflection of each section along the beam in order to define completely the configuration.

Natural frequencies and normal modes of vibration [15]: The number of natural frequencies of vibration of any system is equal to the number of degrees of freedom; thus, any system having distributed parameters has an infinite number of natural frequencies. At a given time, such a system usually vibrates with appreciable amplitude at only a limited number of frequencies, often at only one. With each natural frequency is associated a shape, called the normal or natural mode, which is assumed by the system during free vibration at the frequency. For the fundamental mode, which corresponds to the lowest natural frequency, the supported or fixed points of the system usually are the only nodal points. In the modes of vibration corresponding to the higher natural frequencies of some systems, the nodes often assume complicated patterns. In certain problems involving forced vibrations, it may be necessary to know what the nodal patterns are, since a particular mode usually will not be excited by force acting at a nodal point [17].

First of all and in order to solve the problem of a circular plate with clamped edge, it is necessary to understand the problem of a circular plate with free boundary. The problem of the vibration of a circular plate [16] has been solved by G. Kirchhoff who calculated also the frequencies of several modes of vibration for a plate with free boundary. The exact solution of this problem involves the use of Bessel functions. In the following an approximate solution is developed by means of the Rayleigh-Ritz method, which usually gives for the lowest mode accuracy sufficient for practical applications.

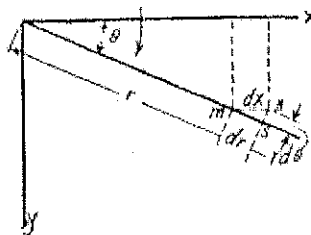


Figure 4-6. Coordinates transformation to Polar coordinates for circular plate calculation

In applying this method it will be useful to transform the expressions for the potential and kinetic energy to polar coordinates [16]. By taking the coordinates as shown in Fig. 5-6, we see from the elemental triangle "mns" that by giving to the coordinate  $x$  a small increase  $dx$  we obtain

$$dr = dx \cos \theta \quad d\theta = -\frac{dx \sin \theta}{r} \quad (4.24)$$

Taking deflection  $v$  as a function of  $r$  and  $\theta$  we obtain,

$$\frac{\partial v}{\partial x} = \frac{\partial v}{\partial r} \frac{\partial r}{\partial x} + \frac{\partial v}{\partial \theta} \frac{\partial \theta}{\partial x} = \frac{\partial v}{\partial r} \cos \theta - \frac{\partial v}{\partial \theta} \frac{\sin \theta}{r} \quad (4.25)$$

In the same manner we will find

$$\frac{\partial v}{\partial y} = \frac{\partial v}{\partial r} \sin \theta + \frac{\partial v}{\partial \theta} \frac{\cos \theta}{r} \quad (4.26)$$

Doing differentiation and substituting in the potential energy of bending for circular plate, we find:

$$V = \frac{D}{2} \int_0^{2\pi} \int_0^a \left\{ \left( \frac{\partial^2 v}{\partial r^2} + \frac{1}{r} \frac{\partial v}{\partial r} + \frac{1}{r^2} \frac{\partial^2 v}{\partial \theta^2} \right)^2 - 2(1-\nu) \frac{\partial^2 v}{\partial r^2} \left( \frac{1}{r} \frac{\partial v}{\partial r} + \frac{1}{r^2} \frac{\partial^2 v}{\partial \theta^2} \right) + 2(1-\nu) \left\{ \frac{\partial}{\partial r} \left( \frac{1}{r} \frac{\partial v}{\partial \theta} \right) \right\}^2 \right\} r d\theta dr \quad (4.27)$$

where "a" denotes the radius of the plate and in the case of a plate clamped at the edge where the deflection is symmetrical about the center:

$$V = \pi D \int_0^a \left( \frac{\partial^2 v}{\partial r^2} + \frac{1}{r} \frac{\partial v}{\partial r} \right)^2 r dr \quad (4.28)$$

The expression for the kinetic energy for same circular plate becomes

$$T = \frac{\pi \rho h}{g} \int_0^a v^2 r dr \quad (4.29)$$

the frequencies of natural modes of vibration for a circular plate clamped at the boundary and symmetrical deformation are calculated by using the Rayleigh-Ritz method

$$\text{Frequency} = p = \frac{\alpha}{a^2} \sqrt{\frac{gD}{\gamma h}} \quad (4.30)$$

In the case of thin plates the mass of the media in which the plate vibrates may affect the frequency considerably. In order to take this into account in the case of the lowest mode of vibration, equation above should be replaced by the following equation

$$p_1 = \frac{10.21}{a^2 \sqrt{1 + \beta}} \sqrt{\frac{gD}{\gamma h}} \quad (4.31)$$

$$\beta = 0.6689 \frac{\gamma_1 a}{\gamma h}$$

Where  $\frac{\gamma_1}{\gamma}$  is the ratio of the density of the media to the density of the material's plate.

#### 4.5 Work done per pressure cycle

The volume displaced by diaphragm can be calculated by using standard assumptions of linear behavior the deflection of a fixed edge, constant thickness diaphragm loaded by transverse pressure is given by:

$$y = \frac{3P(1-\nu^2)}{16Eh^3} (a^2 - r^2)^2 \quad (4.32)$$

where  $y$  is the deflection at radius  $r$ , under applied pressure  $P$ , for a diaphragm of radius  $a$ , thickness  $h$ , Young's Modulus  $E$ , and  $\nu$ . The maximum deflection of the diaphragm which occurs at the center ( $r = 0$ ) is

$$y_0 = \frac{3(1-\nu^2)Pa^4}{16Eh^3} (a^2 - r^2)^2 \quad (4.33)$$

The volume swept by the moving diaphragm is found by integration of equation (4.32)

$$V = (1 - \nu^2) \frac{3\pi P a^6}{48 E h^3} \quad (4.34)$$

Substituting equation (4.33) into (4.34) we find that the swept volume of the diaphragm is related to the maximum deflection and the diaphragm area.

$$V = \frac{\pi a^2 y_0}{3} \quad (4.35)$$

Let's remember that the HPS diaphragm is not totally flat round disc, in the inside part the design alloys stress relief frames (curve shapes) that may change the 1/3 portion of the equation above.

To understand the dynamic response of a diaphragm it is critical that the kinetic and potential energy characteristics of the diaphragm be recognized. Kinetic energy of the diaphragm can be determined in much the same manner as swept volume. For a diaphragm oscillating at fixed radial frequency  $\omega$ , with a deflection profile equal to the static deflection profile, integration will lead to a kinetic energy  $T$ , for the diaphragm [3].

$$T = a^2 \rho h \frac{(\omega y_0)^2}{10} \quad (4.36)$$

Where  $\rho$  is the material's density

For a diaphragm oscillating in a fluid space with significant hydraulic pressure variations the potential energy comprises two components. The first is the potential energy associated with the mechanical energy stored in the deflected diaphragm. Second is the potential energy stored in the compressed fluid in the working chamber. The work done by a diaphragm as the diaphragm moves through a quarter cycle compressing the working liquid is given by the product of force and the distance through which the force acts. However this work contains both the potential energy of the diaphragm and one quarter of the power dissipated ( $D/4$ ) in the thermodynamic cycle being implemented. Knowing the system cycle requirements we can determine the pressures which a diaphragm must generate, and the work required per cycle ( $D$ ).

$$U_{liquid} + \frac{D}{4} = \int_0^{\frac{\pi}{4}} P A dy \quad (4.37)$$

Where  $U_{liquid}$  is the potential energy of the compressed liquid,  $D$  is the work per cycle done on the liquid by the diaphragm,  $P$  is the pressure against which the diaphragm acts, and  $y$  is the deflection of the diaphragm. Knowing the deflection profile of the diaphragm (4.32) and knowing that the pressure,  $P$ , in the work space takes the form

$$P = P_c \sin(\omega t + \phi) \quad (4.38)$$

where  $P_c$  is the amplitude of the pressure swing and  $\phi$  is the phase angle of P relative to deflection  $y$ , the sum of gas space potential energy and one quarter of the cyclic work is

$$U_{liquid} + \frac{D}{4} = \frac{2\pi P_c a^6}{6} \left[ \frac{3(1-\nu^2)P}{16 E h^3} \right] \left( \frac{\cos \phi}{2} + \frac{\pi \sin \phi}{4} \right) \quad (4.39)$$

Substituting for swept volume (4.35)

$$D = \pi P_c V \sin \phi \quad (4.40)$$

So the liquid space potential energy is:

$$U_{liquid} = \frac{V}{2} P_c \cos \phi \quad (4.41)$$

where  $V$  is the volume swept by the diaphragm,  $P_c$  is the pressure amplitude in the working space and  $\phi$  is the phase angle between pressure swing and diaphragm amplitude.

To calculate the potential energy due to the spring effect of the diaphragm itself we simply must realize that a pressure P required to deflect a diaphragm is a direct measure of the spring stiffness of the diaphragm. Thus the potential energy contribution from the diaphragm is

$$U_{diaphragm} = \frac{V}{2} P \quad (4.42)$$

And the total potential energy,  $U$ , is:

$$U = \frac{V}{2} P + \frac{V}{2} P_c \cos \phi$$

Where  $P_c$  is the working space gas pressure amplitude and P is the pressure required to deflect the diaphragm through swept volume V.

## 4.6 Residual stress

Internal stresses are to be considered as the following:

1. Operational strains referring to loads that the material is subject and calculated
2. Residual stresses in the material caused by heat treatments or stresses caused by welding, forging, casting, etc.

Residual stress is usually defined as the stress which remains in mechanical parts which are not subjected to any outside stresses. Residual stress exists in practically all rigid parts, whether metallic or not (wood, polymer, glass, ceramic, etc). It is the result of the metallurgical and mechanical history of each point in the part and the part as a whole during its manufacture. It exists at different levels, generally divided into three, depending on the scale on which the stress is observed:

- 3rd level stress, on the crystal scale. At this level, the outside limit of the notion of stress is reached. It corresponds to the actions created by all the different types of crystalline defects: vacancies, interstitial compounds, substitute atoms, dislocations, stacking defects, twin crystals and grain joints.
- 2nd level stress, due to the heterogeneity and anisotropy of each crystal or grain in a polycrystalline material. In the presence of mechanical stress (uniform traction of a smooth test specimen, for example), certain grains oriented in the right direction will reach the yield point before others, which results in heterogeneous behaviour when the load is eliminated. The resilience will therefore develop differently or more or less freely according to the grains, thus producing non-nil stresses (2nd level residual stress). However, the average of these stresses, that is,

the general resultant along the traction axis, will be nil at the end of the test (1st level residual stress). This type of stress can be measured by X-ray diffraction.

- 1st level or macroscopic residual stress, affecting a large number of grains or the whole of the mechanical part. It can be measured using gauges, for example, which detect the deformation produced, or X-rays.

The origin of the residual stress is mainly given by:

- Plastic deformation causes the surface to become slightly dimpled, so that the surface roughness is increased, which may or may not facilitate crack initiation on the surface.
- Non-homogeneous plastic flow under the action of external treatment (shot-peening, autofretting, roller burnishing, hammer peening, shock laser treatment),
- Plastic working on the surface means that strain hardening occurs, resulting in a change in surface hardness and an increase in the yield stress of the material.
- non-homogeneous plastic deformation during non-uniform heating or cooling (ordinary quenching, moulding of plastics),
- structural deformation from metalworking (heat treatment),
- heterogeneity of a chemical or crystallographic order (nitriding or case hardening),
- various surface treatments (enamelling, nickel-plating, chrome-plating, PVD and CVD coating),
- Differences in expansion coefficients and mechanical incompatibility of the different components of composites (composites with a metallic and organic matrix, ceramic coatings).



- Elastic plastic relaxation of near surface layers as the shot rebounds induces residual compressive stresses parallel to the free surface of the component. The effects of these stresses act to delay crack initiation, and hence hinders crack propagation by alleviating the resultant applied stress.

The residual stress in a metal doesn't depend on its hardness, but from the elasticity module or Young module and from its chemical composition. This stress is part of the metal's elasticity field and has a three axis spatial orientation. The hardness of a metal indicates its ability to absorb elastic or plastic energy, but through it not possible to determine the value of residual stress. In a metal with the same hardness we will have different values of this stress. The residual stresses tend to equilibrate themselves in the surface of the material.

The measurement made with all the major methods, X-ray, string gauge (destructive), optical etc. the residual stress is determined between the measuring the displacement of the equilibrium point the reticule crystalline.

## PART IV. DESIGN

### Chapter 5. Electronic Design

An important part of the HPS is the related to the electronics, however as previously mentioned; it is not pretended to cover the electronic design in this document due to Delphi's Proprietary Information. Besides Delphi, Analog Devices is also protecting the development of the ASIC to be used in this application. Electronic components are commonly completely protected to minimize any exposure to the environment. Exposed parts can degrade or fail because of introduction of contaminants or corrosion. Contaminants can come in, which diffuse into the part and alter electrical characteristics or can cause short circuits, blockage of measure and signal, or interference of required mechanical motion. The HPS electronic compartment, present isolation potting material in order to reduce the risks mentioned above.

#### 5.1 Schematic design

##### 5.1.1 Layout

A principle of operation of the HPS is pretty straight and in order to measure the pressure variations it is needed to:



Figure 5-1. Flow process for capacitance measurement operating principle

As mentioned on Part I, the HPS is a cross functional. The detailed electronic design will not be covered in this thesis, however it is important to show the final results of the magnificent effort that the electronic engineers demonstrated in this project.

By using thick film technology, one of the sides of the ceramic substrate is used to print the capacitance sensing electrodes and the other side is used to print the electrical connection for the electronics. This PCB on a ceramic substrate also called a Hybrid Circuit gives the advantage to use existing parts of the design, and mounting the electronics over the ceramic substrate and avoid additional lead frames to connect electrically the electronics components. This technology also supports the use of Flip Chip Package Technology for the electronics that can helps us optimize the real state area for component placement. By having the electronics next to the sensing element; reduce noise and signal losses, achieving better sensitivity to the measure capacitance and smaller parasitic that affects the performance of the circuit especially over temperature changes.

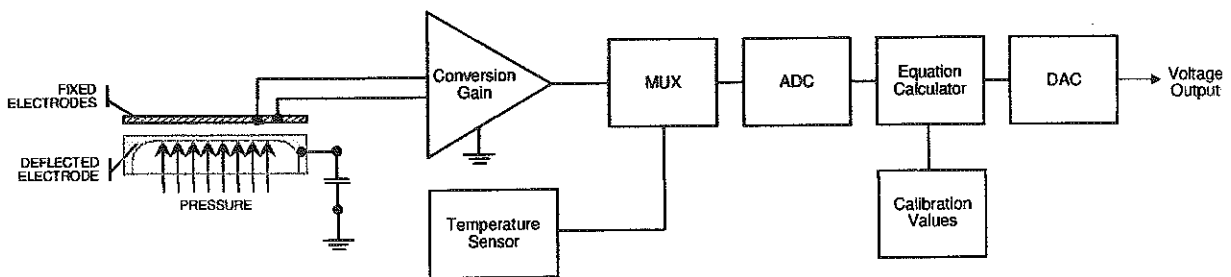


Figure 5-2. Operating principle for electronic design

REFER TO CDR HPS – ADP  
20070312a.PPT

# Analog Devices IC AD7747 Block Diagram

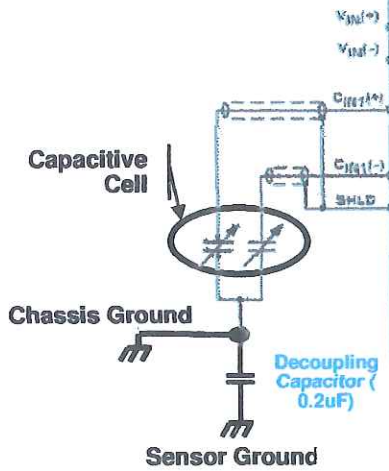


Figure 5-3. Electronic layout for the HPS electronics

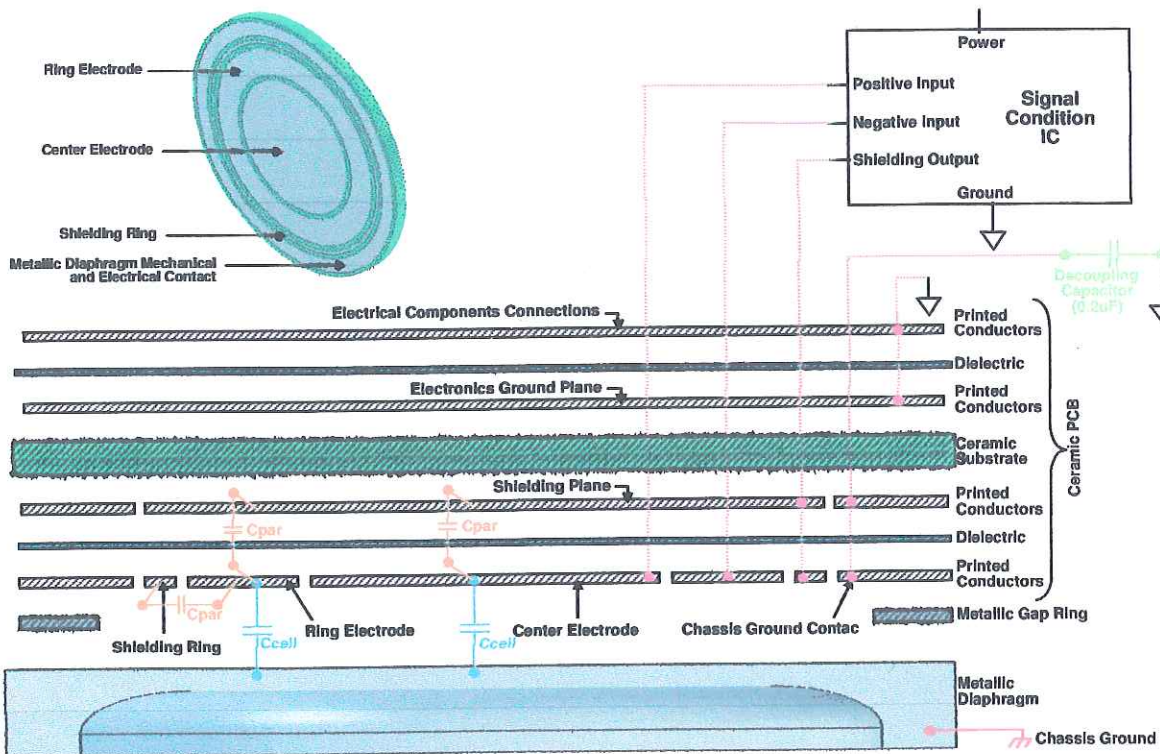


Figure 5-4. Electronic layout for the HPS electronics

### 5.1.2 Predicted response

By mean of mathematical calculation or AC electric field simulation, the predicted capacitance for the HPS sensing element according to hydraulic pressure variations.

Figure 5-5 shows the output curve for the HPS.

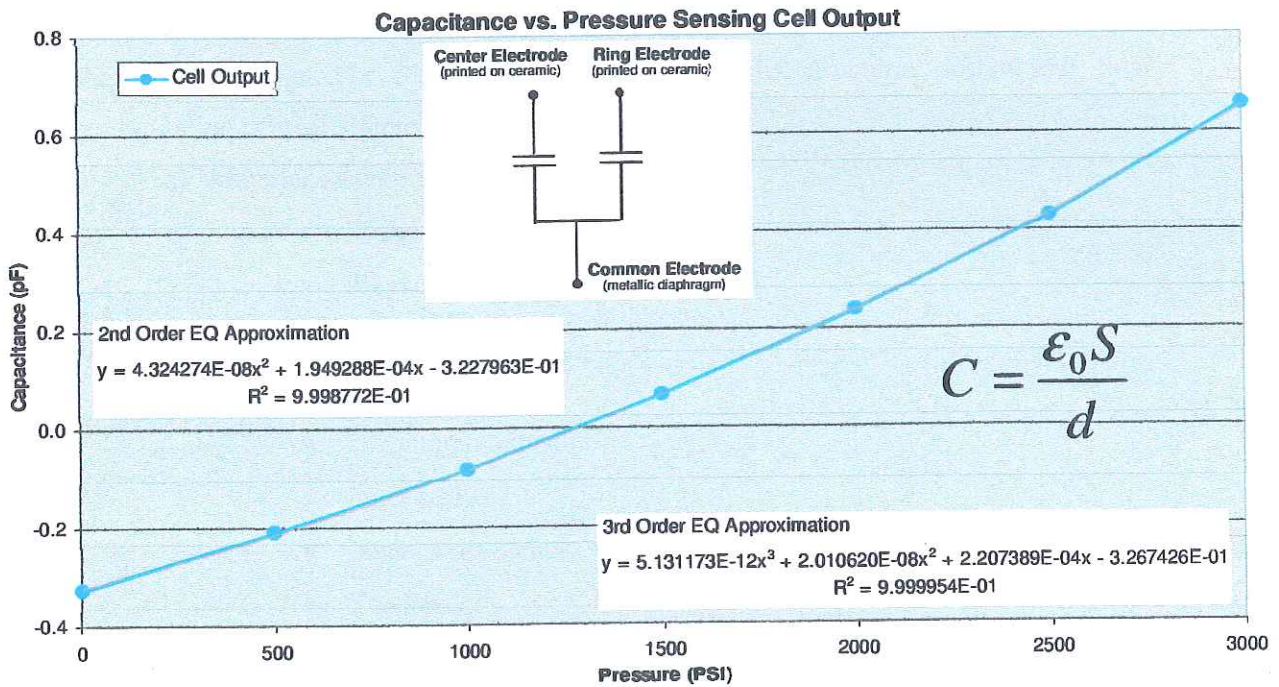


Figure 5-5. Capacitance response for the HPS

## Chapter 6. Structural design

### 6.1 Diaphragm

#### 6.1.1 Preliminary design

Packaging and testing of any new development presents significant challenges. The diaphragm must be designed to withstand the active pressure range (operating and overpressure) and guarantee structural integrity along its infinite cycle life. According to the DFSS (Design For Six Sigma) methodologies Its structural design and final configuration is most affected by:

- a) Material selection
  - Media compatibility
  - Elastic modulus
  - Yield strength
- b) Dimensions
  - Diaphragm diameter
  - Inner radius
  - Inner cavity radius
  - Thickness
- c) Boundary conditions
  - Attachment method
    - Laser
    - Resistance welding
    - Threaded
  - Profile
    - Depth
    - Interference length
- d) Manufacturing process
  - Forming method

These parameters define the final dimensions of the circular and flat diaphragm clamped at the edges according to pressure range. Although it would be possible to create other deflective diaphragm configurations for different pressure ranges (low and ultrahigh pressure levels); it is important to take consideration of the dynamic range that is actually a function of the distance variation between both electrodes; that in this case can be prompted by either varying the gap or increasing the diaphragm deflection -the larger Dynamic Range, the larger Diaphragm's Deflection- ; however there are some other alternatives that can be implemented in order to achieve better dynamic range for those designs with minimum deflection (See Chapter 9).

a) Material selection

Preliminary material evaluation was conducted in order to select the right material for the HPS (Refer to ADP HPS 3000 PSI DFSS # 26286). Some of the basic questions to end up with the material selection were related to the machinability, formability, weldability, environment, service life, media compatibility, cost, availability, stock size and temper to manufacture the lowest finished part cost. Mainly, the infinity cycle life and expected diaphragm performance must be guarantee at all operative conditions even when harsh environment is present. There is not written specification to survive infinite cycle life for the diaphragm design so it was used a rule of thumb for ductile materials: The maximum stress on the part should be about 50% of the yield strength. In addition and in order to obtain good fatigue life (a million cycles or more) to account for material properties and weld depth variability, the maximum recommended pressure load should then be limited no more than 80% of the maximum load obtained for infinite cycle life (Refer to Delphi's Memo #m04\_072).

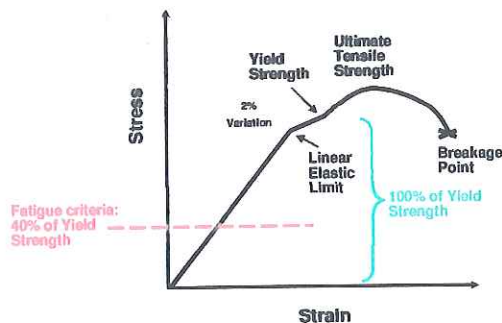


Figure 6-1. Stress vs strain representation showing 40% of Yield to guarantee cycling endurance

For the HPS Diaphragm's, the maximum permissible stress was fixed to 40% of the yield strength –for the flat and circular shape clamped at the edge-. The recommended material for the HPS diaphragm's is Carpenter Project 70+ @Condition 900 with the following characteristics:

Material: 17-4 PH

Elastic modulus 193 e3 MPa

Poisson's ratio: 0.272

Yield strength: 1170 MPa

Due to variability of nominal properties based on different bibliography –even manufacture can not guarantee a nominal value- it was necessary to conduct a tensile test for the material above to determine the minimum yield value that can actually be used as nominal for the diaphragm design (Refer to Centro de Investigacion en Materiales Avanzados –CIMAV- report #07/0318A). Also, besides to the batch to batch variation; most materials are temperature sensitive, so the sensitivity of the diaphragm will increase with temperature variations. At elevated temperature the yield strength falls, while at low temperature notch sensitive increases [3].

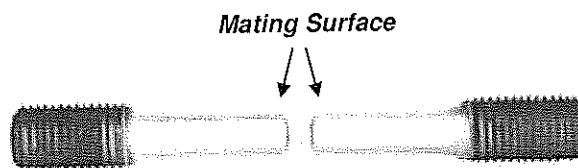


Figure 6-2. Notched tensile specimen showing location of fracture. SS 17-4 PH Heat treated 900 condition



## b) Dimensions

Based on Finite Element Analysis simulations (FEA) and statistical analysis conducting Design Of Experiments (DOE), it was concluded that the final geometry and main dimensions that affect the stress and deflection behavior for a flat circular diaphragm welded at the edge are:

- Thickness
- Inner radius
- Outer diameter
- Height
- Welded joint is fixed (Laser weld) according to preliminary assessment (refer to Miyachi Unitek report: Application number 6613)

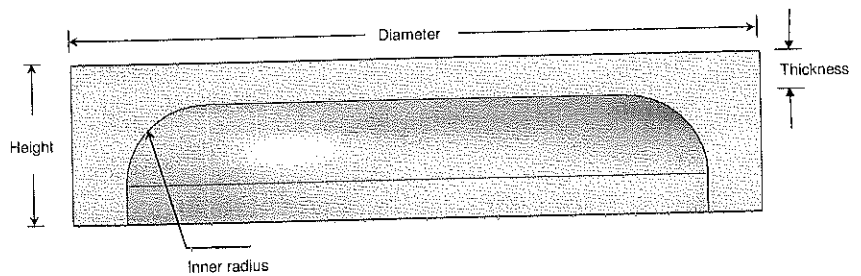


Figure 6-3. Cross section view of flat diaphragm

The preliminary assessment ends up with strong influence of thickness over deflection and stress. It was also included the tolerances analysis ( $\pm 0.08$  mm) to guarantee to do not overstress the diaphragm for those conditions where Minimal Material Condition (MMC) is present.

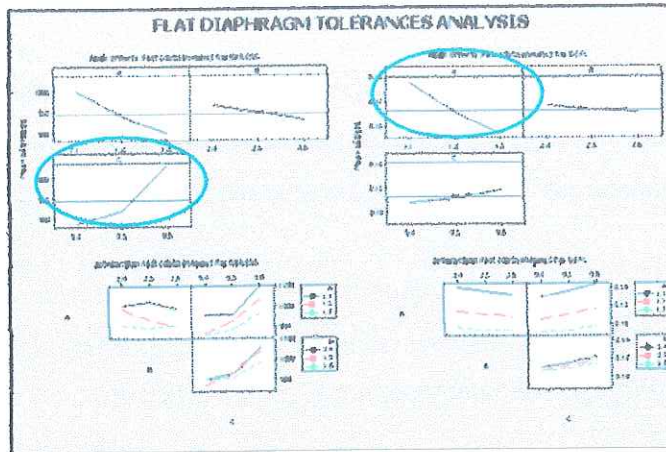


Figure 6-4. DOE for flat diaphragm demonstrates that thickness is the main factor

### c) Boundary conditions

Several attachment approaches were analyzed for implementation for the HPS, those designs were oriented to full fit the attachment requirements between the base port and diaphragm: Some of these designs were built and tested as prototypes samples (ADRW and Laser), other were only analyzed (press fit and threaded interfaces).

- The greater interface the better
- Reduce secondary process to create interference
- Reduce cost equipment investment
- If same material, meet melting point for both parts as much as possible for welding process
- Reduce additional post-process to finalize part and restore material properties

Annular Deformation Resistance Welding (ADRW) technology (Fig 6-5 and 6-6) was first selection due to:

- Benefits
  - Delphi's ownership technology
  - Low initial investment
  - Less time consuming
  - Different metals can be welded
  - May be suitable for those designs where cost reduction is based on material cost/availability

- Disadvantages
  - Interference configuration increase the price of the diaphragm
  - Interface area affects material properties surround the weld area
  - Additional secondary process is needed to recover material properties

The principle of operation of the ADRW is to apply straight pressure (perpendicular to surface preferable) between the components to be welded while an electric current flows through them. The final product consists of a melted joint having the material properties stronger than the softer metal.

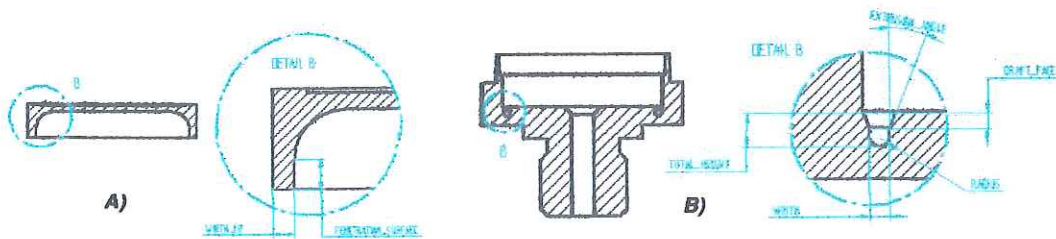


Figure 6-5. Annular Deformation Resistance Welding (ADRW) A) Diaphragm and B) Baseport configurations

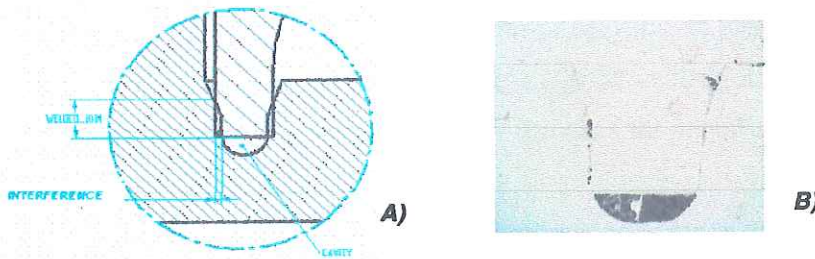


Figure 6-6. Annular Deformation Resistance Welding (ADRW) cross section view A) Detailed drawing interference and B) Prototype part

Laser weld technology (Fig 6-7) was considered due to:

- Benefits
  - Well known process
  - Low cost initial investment
  - Not big impact in material properties of the surrounding areas
  - High accurate welded joint

▪ Disadvantages

- Reduced area of interference
- Same or similar Stainless Steel must be welded
- Weld splatter over top surface

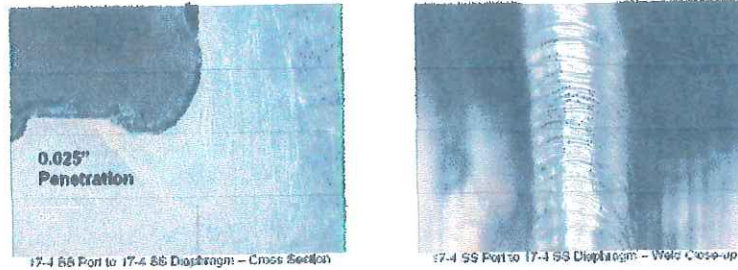


Figure 6-7. Laser weld cross and plain views of prototype parts

d) Manufacturing process

Materials used to built diaphragm and base port for HPS, must not be too soft nor too hard because soft materials tend to tear and give poor finish. The hard materials may increase the cost of production due to take longer time for machining process. Even when there are so-called free-machining alloys contain sulfur or selenium in more than required quantities, it makes the material incapable of producing a good welded joint.

Also, excessive work hardening is not desirable as it makes the metal too brittle, thus secondary annealing must be applied.

Basically, the general requirements must meet the final part in order to guarantee proper installation and functionality:

- Low cost
- Dimensional stability against temperature variation
- Flatness over top of diaphragm
- $\pm 0.08\text{mm}$  tolerance
- Surface finish not above  $0.025\text{mm}$  tolerance
- If secondary process needed –post heat treatment- distortion is not allowed

Four processes were considered to manufacture the diaphragm:

- Stamping. Low cost but may not guarantee flatness.
- Deep Drawn. Low cost but is not feasible for desirables shape and dimensions.
- Metal Injection Molding. Low cost but guarantees only 90% of material properties and porosity is present.
- Machining. Accurate but may be the highest cost.

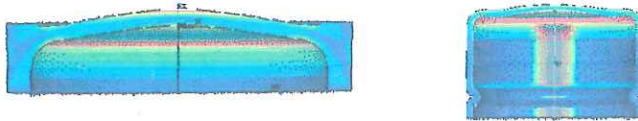


Figure 6-8 Preliminary assessment before run prototyping built for Machined and Stamped diaphragms

The machining process presents more dimensional accuracy over other process. Stamping is also suitable and according to FEA, could demonstrate higher deflection with the same stress ratio (See 6.1.2); however the final sensor packaging may jeopardized the dimensional stability of the flat surface needed to obtain the differential capacitance measurement. If deflection of flat surface is fixed and actually can be limited to low ranges (1.5x compared with machined part) and further development for final packaging, then this stamped option may be suitable for soft materials, to reduce the cost of the diaphragm; unfortunately it is needed a high initial cost for tooling in order to build prototypes and run a quick proof of concept.

#### 6.1.2 Predicted stress/deflection ratios

As mentioned before, during the design of the pressure sensor, the diaphragm had several approaches according to potential packaging design (See Chapter 7). The way to proof the deflection of the diaphragm for the HPS was done on early stages of the project by mean of construction of dummy diaphragms prototypes (Fig 6-9) where two different materials were used Cooper beryllium and SS 317 tested at ambient condition.

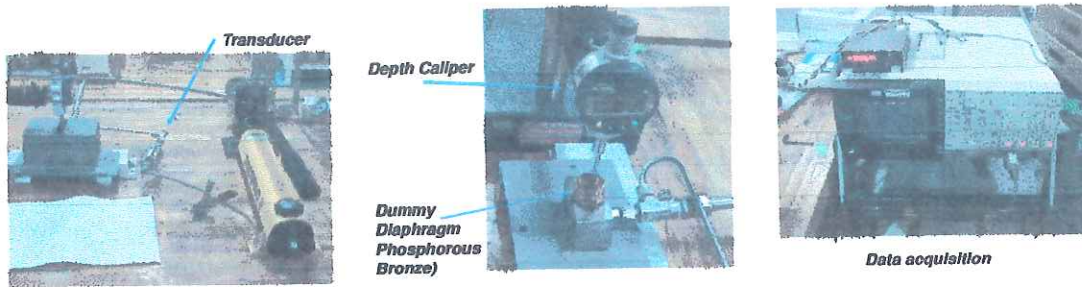


Figure 6-9. Set up for proof of deflection test

Material	Pressure (PSI)	FEA (mm)	Sample One (mm)	Sample Two (mm)
Cooper Beryllium	2000	0.033	0.037	0.036
SS 317	2000	0.010	0.010	0.011

Table 2. Numerical comparison between FEA and two different real parts

As can be seen on Table 2. There is a close correlation between the FEA model and the real reading for both samples, so for the prototype sampling, the current FEA model was used and modified according to different dimensions of thickness and radius in order to meet the pressure requirements.

A 3D quarter-symmetry stress analysis of the metallic diaphragm was performed using second order tetrahedral elements for different diaphragms' dimensions and symmetry faces constrained having the consideration to simulate a clamped diaphragm (weld region fixed) with isotropic behavior (Fig 6-10 and 6-11). It would also be possible to perform a 2D FEA modeling that actually reduce the simulation time instead of a 3D simulation, however due to the availability of the 3D parasolid models it was preferred to take advantage of it. For structural modal model in 2D, it is suggested to use harmonic elements such as PLANE25.

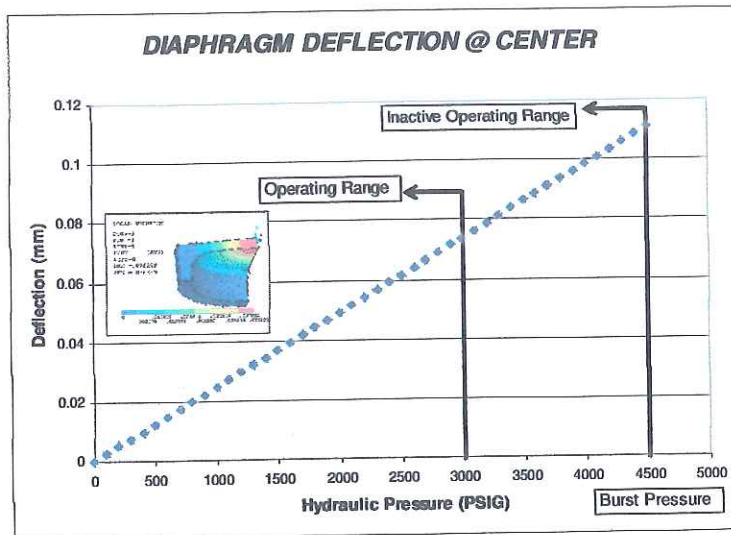


Figure 6-10. Predicted deflection at center of diaphragm based on FEA for not optimized diaphragm

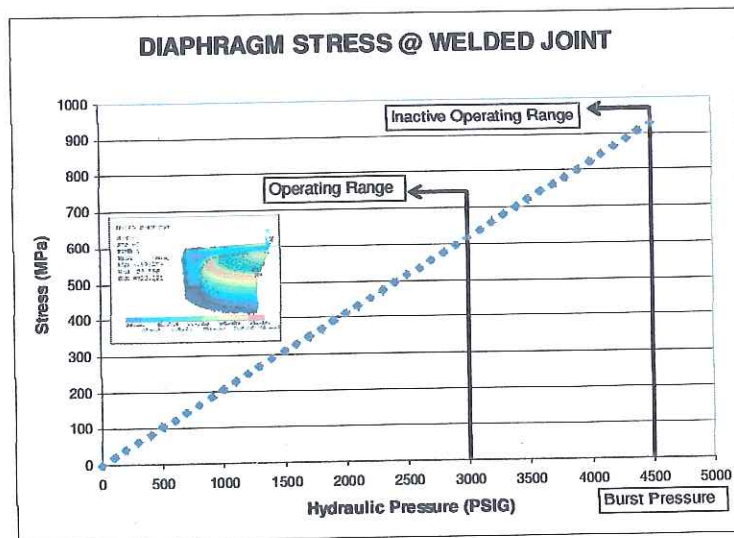


Figure 6-11. Predicted stress located at inner radius based on FEA for not optimized diaphragm

For subsequent analyses, it was necessary to include the tolerances variation and temperature effect to conclude with the final dimensions of the HPS Diaphragm (Reference DELPHI HPS-ADP CDR -03-20-07). The stress/deflection ratios for the diaphragm are included in table 3.

Maximum Deflection @ 3000 PSI: 0.05 mm
Maximum Stress @ 3000 PSI: 482 MPa

Table 3. Stress/Deflection prediction @3000 PSI for the deflective diaphragm

- Solder joint thermal analysis

Overmold connector (three pins) was used on the HPS. Unknown thermal growth that may jeopardize the integrity of a solder joint that actually must provide all time electrical interface and structural attachment to terminals and pads. A 3D thermal-stress model analysis of the assembly was performed using second order tetrahedral elements for a FEA. Coupling, contact and thermal-stress models were used as a mathematical base for this analysis. No tolerances were included in this simulation, a complete tight fit and full weld penetration between terminals and pads as well as high tangential forces due to the over mold of housing and terminals. The bottom and lateral faces of the three pads were constrained in all directions. This analysis was done at a range of two different temperatures, the first case for those changes at  $-40^{\circ}\text{C}$  and the second for those changes at  $125^{\circ}\text{C}$ .

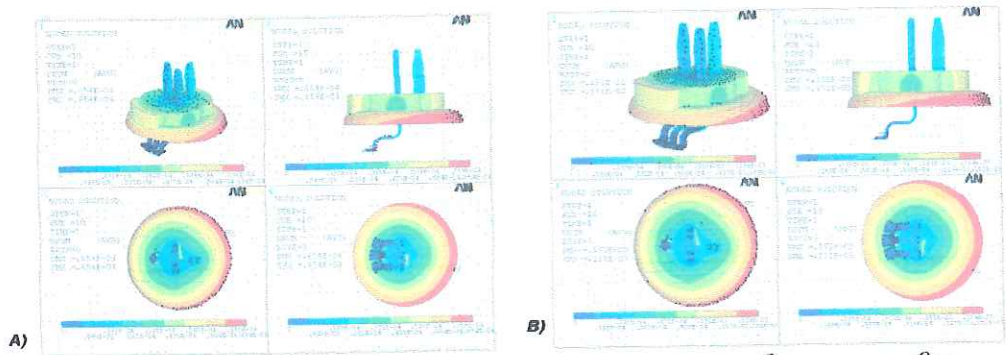


Figure 6-12. Predicted thermal stress on overmold connector A)  $-40^{\circ}\text{C}$  and B)  $125^{\circ}\text{C}$

Based on simulation results, there is not big impact of the thermal stress over the pads since the Tensile Strength for this material is 338 MPa and our highest value is 0.0128 MPa at  $125^{\circ}\text{C}$ . Also the results show that the force on the weld will not affect the integrity of the solder joint ( $-1.43\text{e-}09\text{ N}$  highest value at  $125^{\circ}\text{C}$ ). The total displacements for each component are also seen to be nearly the same. However, due to the larger



temperature differential between the lowest ( $-40^{\circ}\text{C}$ ) and the highest ( $125^{\circ}\text{C}$ ), the  $125^{\circ}\text{C}$  will cause the most thermal impact of the assembly based on the Von Misses Stress values.

Temp $^{\circ}\text{C}$	Displacement m		Stress Mpa	
	-40	125	-40	125
Housing	8.54E-05	1.51E-04	0.8991	0.7095
Terminals	2.34E-05	4.10E-05	1.155	2.019
Solder Joint	3.15E-07	5.55E-07	0.1346	0.2363
Pad	5.04E-10	8.85E-10	0.073	0.0128

Temp $^{\circ}\text{C}$	Total Force on pads N	
	-40	125
Left	-4.04E-10	6.72E-10
Central	7.98E-10	-1.43E-09
Righth	-4.51E-10	7.58E-10

Table 3. Predicted thermal growth values

## Chapter 7. Concepts generation

### 7.1 Mechanizations

In order to explore and develop concepts alternatives as part of Design Process (including overall sensor mechanization), it is important to understand the costumer needs.

Based on a Design For Six Sigma (DFSS) methodology (Refer to ADP HPS 3000 PSI DFSS Plan/Report 26286), the Voice Of the Costumer (VOC) can be translated into engineering requirements according to the House of Quality (HOQ) or Quality Function Deployment (QFD).

- The QFD1 comes up with results to guide future efforts toward deploying the Voice Of the Customer (VOC) into the design and technical actions (Fig 7-1).
- The QFD2 ties together the costumer domain with the engineering needs based on the results of the QFD1.

The first part of the QFD exercise is the solution of the QFD1 based on the Customer Domain. Due to Delphi's proprietary information, there will be not further explanation of the QFD1 Inputs and Outputs.

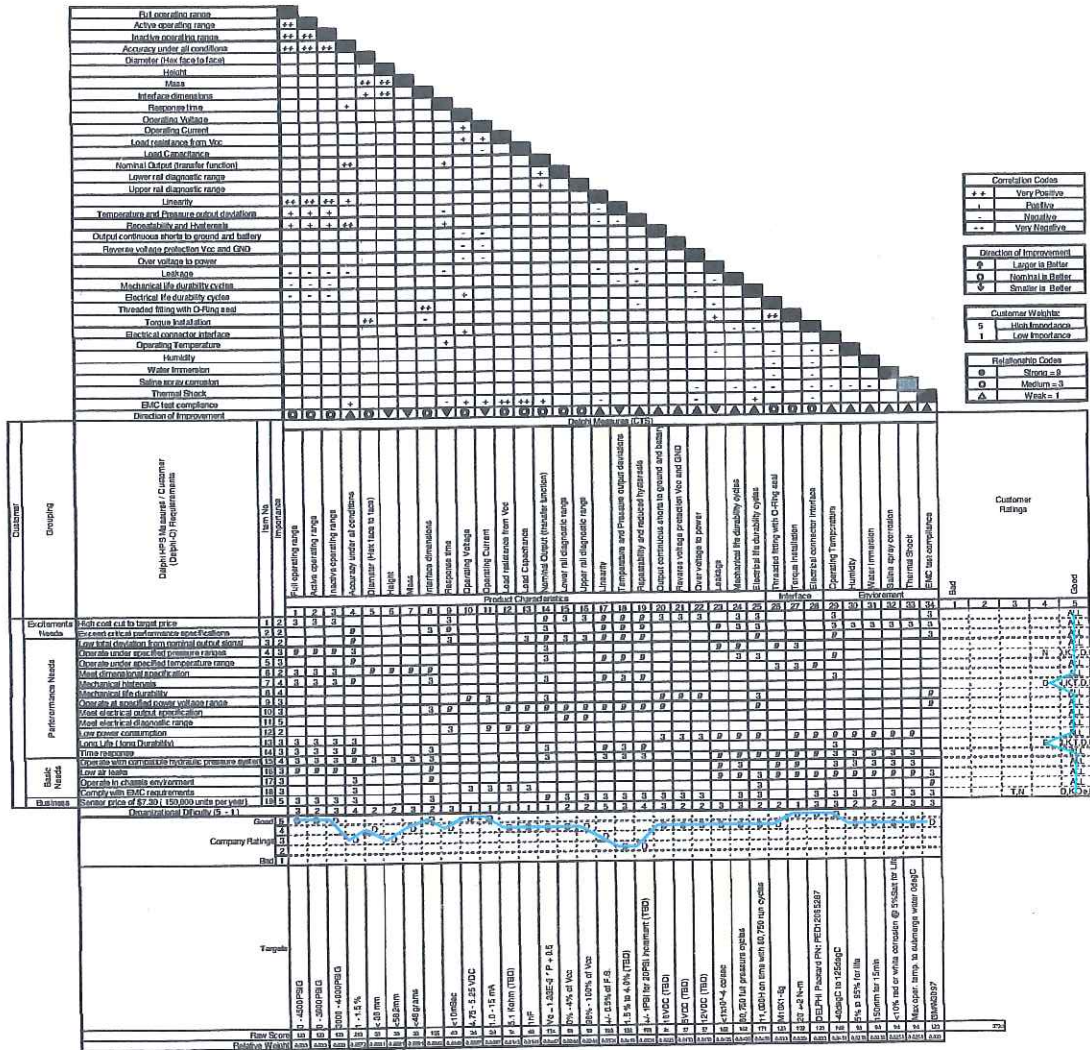


Figure 7-1. QFD1 for HPS assembly

The QFD 2 prioritizes the Functional Requirements (FR's) that define the design for the HPS to achieve the customer satisfaction. Also, the basic functions are the minimum number of functions necessary to address the CT's

Delphi Measures (CTS)		Functional Requirements															Technical Target							
		Item No.	1	2	3	4	5	6	7	8	9	10	11	12	13	14		15						
Product Characteristics	Accuracy under all conditions	1	5	2														±1 - 1.5%						
	Nominal Output (transfer function)	2	3	3	1	3												$V_0 = 1.33E-3 * P + 0.6$						
	Linearity	3	5	1		3												±0.05% of F.S.						
	Temperature and Pressure output deviations	4	3	1	1													±1.5% to 4.0% (TBD)						
	Repeatability and Hysteresis	5	4	1	1		3	3										±1 PSI for 200 PSI increment						
	Leakage	6	5					3	3									<1x10 <sup>-4</sup> cc/sec						
	Full operating range	7	5			3	1		3	3								0 - 4500 PSI						
	Active operating range	8	5	1					1	1								0 - 3000 PSI						
	Inactive operating range	9	4							1	1							3000 - 4500 PSI						
	Mechanical life durability cycles	10	5				1	3										80,750 full pressure cycles						
Interface dimensions	11	3						3									100 MTO 2, 1-6G							
Electrical life durability cycles	12	4															11,000H on base with 60,750 run cycles							
Operational Temperature	13	3	1	1	3												-40degC to 125degC							
EMC test compliance	14	3															GMV3007							
Constraints	Survives 23 years of service																							
Noise	0.5D USD																							
	Attachment method																							
	Material Yield strength																							
Functional Targets		0 - 3000 PSI	0.5 FF	0.45cm <sup>3</sup> /0.25m <sup>3</sup>	0.03 mm	3 mm	14.7 PSI	0.03 - 0.07 mm	<1 x 10 <sup>-4</sup> cc/line	1.0 - 16 m/s	1100 Alpha	0.01 mm Adjust 0.1µg	300 Kg	<600 Mpa	<6 N	<20 mm	DELPHI Predicted FNL P	1.5% to 4.0%	DELPHI Predicted FNL P	7 x 10 <sup>-5</sup> /degC	0.07 mm Adjust. 1 µg	<1 Mpa	<5 m/year	
Row Score	44	61	66	65	59	66	66	66	66	65	67	67	64	61	61	64	64	54	69	65	65	62	67	61
Relative Weight	0.03	0.04	0.04	0.05	0.03	0.05	0.05	0.05	0.05	0.03	0.05	0.05	0.09	0.09	0.05	0.05	0.05	0.05	0.05	0.04	0.04	0.04	0.04	0.05

Figure 7-2. QFD2 for HPS assembly

The outputs of the QFD2 are those minimum FR's to guarantee the proper functionality of the system and help to define the Design Parameters (DP's) that actually drive technically the design of the sensor. The basic functions are the minimum number of functions necessary to address the CT's. The conclusion of this design stage is to demonstrate that the design space have a strength relation with the customer domain.

The goal of the DFSS methodology is to provide a way that actually guarantees not conflict between functions of the product. This is important to demonstrate not conflict or interaction between the Design Domain and Function Domain based on the use of the Axiomatic Design.

The Axiomatic Design analysis is used to correlate a FR with a DP:

- FRs are defined followed by the selection/definition of the DPs
- Goal is an un-coupled design (Path Independence) to create a robust design
  - Satisfy the Independence Axiom
  - Each function controlled by one design parameter (FR – DP)
  - Coupling in DP map influence the approach
- If it is present, resolve coupling issue

	DP 0 - Capacitive Sensor	DP 1 - Metallo Hexapram	DP 1.1 - Laser sensor to base port interface	DP 1.2 - Boundary attachment	DP 1.3 - Air gap cavity design geometry	DP 1.4 - Within hexapram requirements	DP 2 - Electronics	DP 2.1 - Capacitive cell	DP 2.2 - ASIC Signal Conditioning	DP 2.3 - Output pins	DP 2.4 - Hybrid circuit	DP 3 - Pin connector	DP 3.1 - Crimping	DP 3.2 - Terminal placement	DP 3.3 - Shear weld terminal/Flex circuit	DP 3.4 - Pairing material	DP 3.5 - Shear weld terminal over ceramic board	DP 4 - Threaded port attachment	DP 4.1 - Metal to metal geometry
FR 0 - Convert hydraulic pressure to digital signal	X																		
FR 1 - Convert hydraulic pressure into mechanical deflection		X																	
FR 1.1 - Seal fuel within chamber			X																
FR 1.2 - Support reaction load				X															
FR 1.3 - Provides a flatness surface					X														
FR 1.4 - Deflection inside elastic range				X		X													
FR 2 - Convert mechanical deflection to digital signal							X												
FR 2.1 - Convert mechanical deflection to capacitance								X											
FR 2.2 - Convert capacitance to electrical signal									X										
FR 2.3 - Condition Electrical signal to Electrical signal output ECM										X									
FR 2.4 - Mount electronic board and second electrode											X								
FR 3 - Provide digital signal to ECM												X							
FR 3.1 - Attach connector to base port													X						
FR 3.2 - Provide electrical connection to pins														X					
FR 3.3 - Make flexible connection from electronics to connector															X				
FR 3.4 - Protects electronics from environment, moisture and water intrusion																X			
FR 3.5 - Provides ambient pressure for usage measurement																	X		
FR 4 - Provides attachment to fuel rail																		X	
FR 4.1 - Seal fuel from atmosphere																			X

Figure 7-3. Mapping FR's to DP's for HPS at sensor level

Implementing an Axiomatic Design analysis at sensor level for the HPS, (Fig 7-3), we can understand that:

- The DP map shows de-coupled design where most functions are independent (diagonal)
  - Function 1.2 & 1.4 dependent on two design parameters:
  - Changes in DP 1.4 effect only FR 1.4
  - Changes in DP 1.2 effect both FR 1.2 & FR 1.4

Based on the previous observations, there are some solutions we can implement:

- Resolve coupling issue
  - Set FR 1.4 to achieve DP 1.4
  - Fix DP 1.2 Boundary attachment per Bill Of Design (BOD) to use it on FR 1.2
    - The attachment profile needs to be considered as part of the diaphragm design

Even when there is a coupling issue, we can implement the solutions above and solve the coupling issue. We can succeed easily and it is clear that there is a potential successful to guarantee the customer requirements based on the design parameters as mentioned above.

### 7.1.1 Bill of design for concepts 1 to 7

Once understood what the customer wants and along the development of the project (Design Stage), there are seven potential mechanization to consider as final trial of the HPS and further evaluation will be presented at the end of this section.

- **Concept One.**

Was developed on early stages of TDP 500 PSI and the mechanical assembly consist of a base port to interconnect with system and hex head diaphragm.

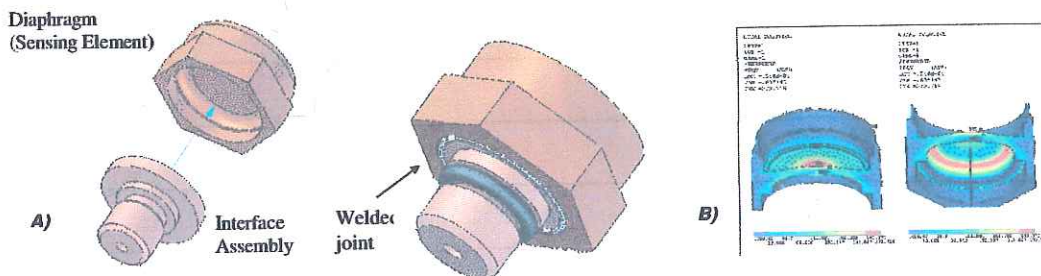


Figure 7-4. A) Interconnection scheme. B) FEA for Option One

- **Concept Two**

Based on experience and ownership of ADRW, this concept was carried out to initiate activities at ADP stage (Refer to DELPHI HPS-ADP CDR -03-20-07). Even when two different metals can be welded –that actually can help to reduce the sensor cost-, secondary heat treatment is needed in order to restore material properties of diaphragm.

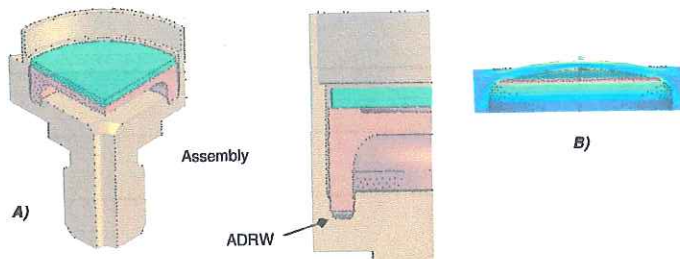


Figure 7-5. A) Assembly scheme. B) FEA for Option Two

- Concept Three/Four

In order to reduce the Bill Of Process (BOP), this concept was developed to reduce process steps and eventually the assembly cost as well. This concept presents a high manufacturability benefit, however and during brainstorming sessions; it was concluded that possible deformation on diaphragm (bending diaphragm under lateral pressure) may challenged the integrity and linearity of the output reading.

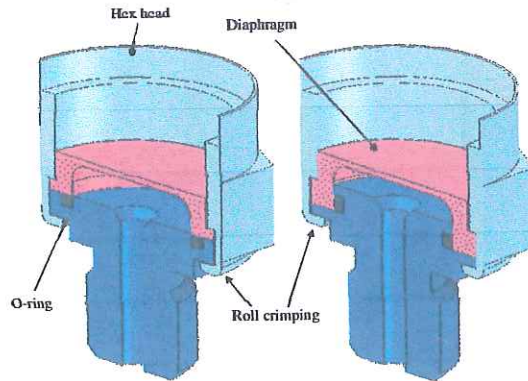


Figure 7-6. Two different concepts based on Roll Crimping mechanization

- Concept Five

Was designed to achieve larger deflection (increase dynamic range) and reduce manufacturing cost. Basically consists of three components: Sheet metal diaphragm, shell rod and hex baseport. The assembly is simpler and low cost; however, the diaphragm which become unstable and snap forward without any additional pressure along time.

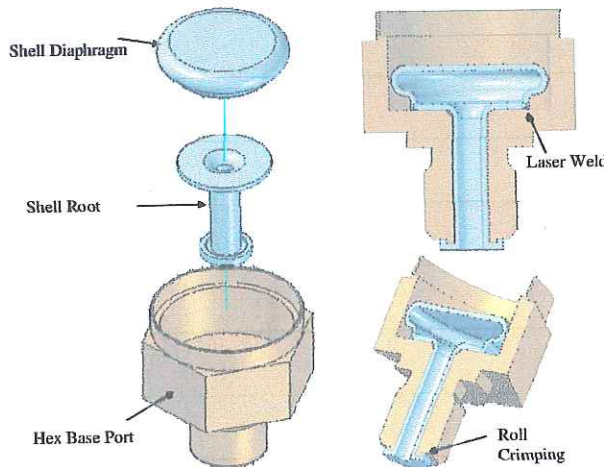


Figure 7-7. Sheet metal option

- Concept Six

The diaphragm design is highly recommended and costly attractive for low pressure ranges due to versatility and benefits of thin sheet metal. However, lack of flatness over diaphragm surface jeopardized the output signal; in addition, initial investment is needed for tooling development.

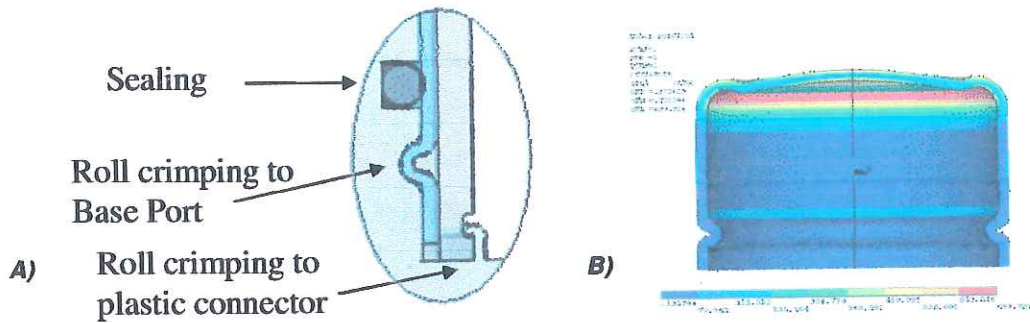


Figure 7-8. A) Interconnection scheme. B) FEA for Sheet metal diaphragm Option Six

- Concept Seven

This configuration was used on proof of concept stage of the ADP project (Refer to DELPHI HPS-ADP CDR -03-20-07). Good performance and laser weld over edge of diaphragm in order to withstand the reaction load and provide sealing from ambient. Can also, achieve two diaphragm's options (Step and flat diaphragm).

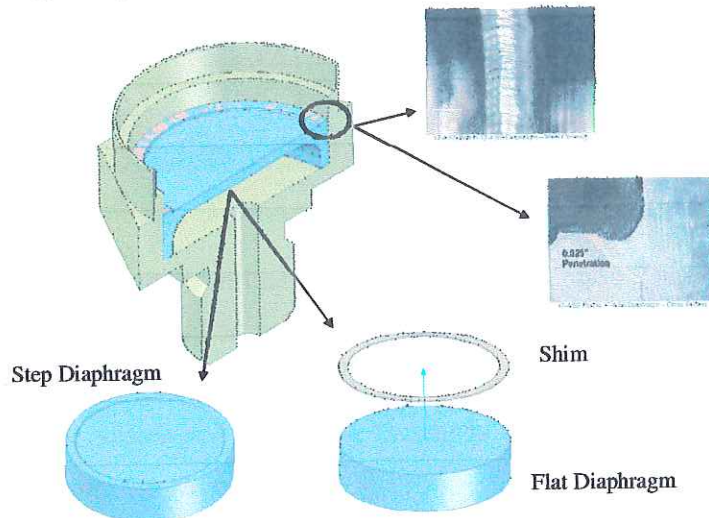


Figure 7-9. Interconnection scheme for Option Seven for Step and Flat diaphragm



All of the options must be deeply analyzed individually; they must meet the same evaluation under the same criteria. The Pugh Analysis provides the sufficient resulting information for evaluating multiple options against each other, in relation to a baseline option (Datum). The method was invented by Stuart Pugh, University of Strathclyde in Glasgow, Scotland as an approach for selecting concept alternatives.

The criteria were picked from the Critical To Satisfaction (CTS's) table (Section 3.1.3) plus additional technical data that may be able to provide additional information related to the system application. Ranking the criteria further helps focus the team's efforts on the critical few. The most strength (+) the best option to select; in the HPS exercise; Laser weld and ADRW presented the best choices for further development.

Concept	Negative	TOP 1	ADRW	CONCEPT 1	CONCEPT 2	DRILL	GAP	LASER	B	ADVANCED
CTSs										
High cost cut to target price		+	+	+	+	+	+	+	S	
Exceed critical performance specifications		S	S	S	S	S	S	S	S	
Low total deviation from nominal output signal		S	S	S	S	S	S	S	S	
Operate under specified pressure ranges		S	S	-	-	-	-	S	S	
Operate under specified temperature range		S	S	S	S	S	S	S	S	
Meet dimensional specification		S	S	S	S	S	-	S	S	
Mechanical hysteresis		S	S	S	S	S	S	S	S	
Operate at specified power voltage range		S	S	S	S	S	S	S	S	
Meet electrical output specification		S	S	S	S	S	S	S	S	
Meet electrical diagnostic range		S	S	S	S	S	S	S	S	
Low power consumption		S	S	S	S	S	S	S	S	
Long Life ( long Durability)		S	S	S	S	S	S	S	S	
Operate with pneumatic pressure system		S	S	S	S	S	S	S	S	
Low air leaks		S	S	S	S	S	S	S	S	
Operate in chassis environment		S	S	S	S	S	S	S	S	
Comply with EMC requirements		S	S	S	S	S	S	S	S	
Sensor price of \$7.30 ( 150,000 units per year).		+	+	+	+	+	+	+	S	
Accuracy under all conditions		S	S	S	S	S	S	S	S	
Nominal Output (transfer function)		S	S	S	S	S	S	S	S	
Linearity		S	S	S	S	S	S	S	S	
Temperature and Pressure output deviations		S	S	S	S	S	S	S	S	
Electrical life durability cycles		S	S	S	S	S	S	S	S	
		1	1	1	1	1	1	1	1	1
		0	0	1	1	1	2	0	0	0
		15	15	14	14	14	13	17	17	0

Figure 7-10. Pugh analysis for HPS concept selection against Datum (Potential supplier)

Rather than simply listing the positive and negative aspects of each option, one by one, a matrix of the needs vs. concepts helps address multiple factors at the same time and gives the team a holistic view of the needs vs. alternatives at hand. Let's remember that the time it takes to analyze the scores and weighting factors is usually much shorter and cheaper compared to deploying the wrong solution.

## PART V. RESULTS AND DISCUSSION

### Chapter 8. Testing and experimental results

It is pretended to present a general explanation of the representative test that will represent the behavior, output characteristics and general trends of the sensor.

The selected mechanization was the Option 7 (See 7.1.1) and several prototypes were built and separated at different batches to proceed with the different scheduled test (Refer to DELPHI HPS-ADP CDR -03-20-07).

- a) Highly Accelerated Test (HALT). This test is conducted to emphasize potential failures of the sensor without pressure and applying gradually the following parameters:
  - High temperature soak
  - Low temperature soak
  - Temperature cycling
  - Mechanical vibration
  - Mechanical vibration with temperature cycling
  - Pressure cycling
- b) Salt Fog. In order to visualize the potential failure by 7 days (without pressure and power); this test is important to analyze that the sealing and corrosion resistance materials withstand harsh environment such as 5% salt @ 32<sup>o</sup> C
- c) Vibration. Apply three axes vibration under specific pulse profile to determine the degradation of both structural integrity and electrical signal. If design is lack of robustness, the performance degradation will be immediately present.
- d) Endurance. Combination of pressure test and thermal cycling is oriented to demonstrate the functionality of the sensor and no degradation of the performance under certain testing profile for a confidence level.

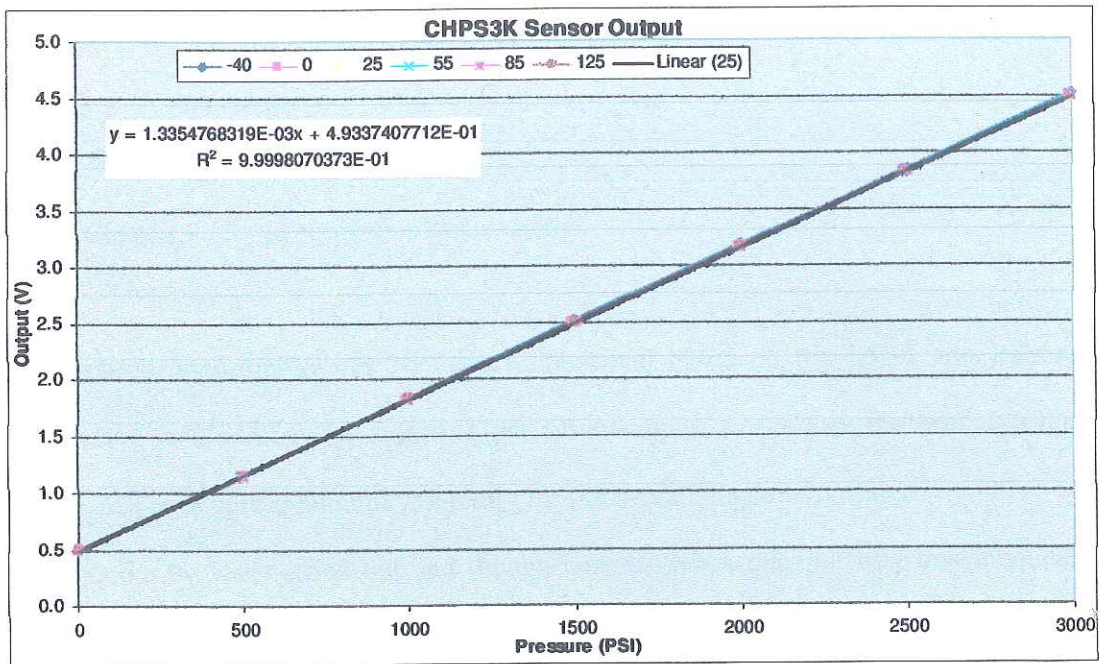


Figure 8-1. Compensated and linearized HPS output @ Temperature

The final results of these tests concluded the confirmation of a good structural integrity and did not impact the performance of the sensor (Refer to DELPHI HPS-ADP CDR -03-20-07).

## PART VI. CONCLUSIONS

### Chapter 9. Optimization opportunities

Optimization opportunities for HPS were conducted based on the DFSS and Robust Engineering methodology by adjusting the system inputs to produce the best possible average response with minimum variability for the overall diaphragm design.

The opportunity was carried out and though because when manipulating mathematical models lend themselves to optimization whereas simulation models require trial and error for optimization.

#### 1. Axiomatic Design provides information to:

- Resolve coupling issue
  - Set FR 1.4 to achieve DP 1.4
  - Fix DP 1.2 Boundary attachment per BOD to use it on FR 1.2
- Use TRIZ and conduct brainstorm session to come up with more alternatives for sealing, boundary attachment and configuration to resolve issue. The potential results will be more applicable for further pressure sensor devices at higher pressure ranges.
- Include high RPN's issues from DFMEA

- Optimize deflection at maximum pressure (burst pressure) to maximize linearity in output signal by changing diaphragm thickness and do not over yield material
- Fix packaging design

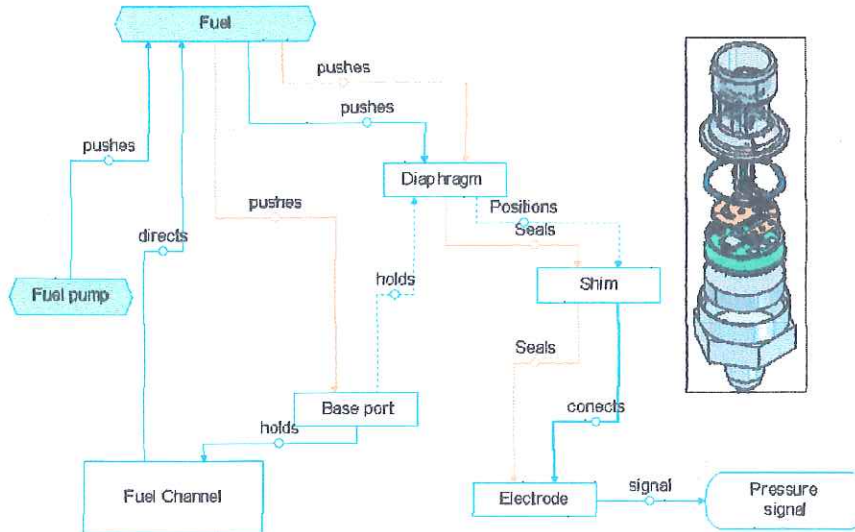


Figure 9-1. Axiomatic Design. Functional Attribute Analysis HPS

## 2. Technical Contradiction

TC1: When the fuel pressure pushes against diaphragm to generate signal it also Pushes against the diaphragm edge and the base port and causes a fuel leak which is undesirable

TC2: If fluid (fuel) does not push against the diaphragm then it will not produce the pressure signal but it would also not cause a leak

TC3: We want to attach the diaphragm against the base port for sealing purposes so the fuel wont leak causes problems with manufacturing and added cost and reliability

TC4. Gap is needed because creates a difference in capacitance between two parallel electrodes

TC5. If sensitivity gets better by reducing the air-gap or increasing the deflection of the diaphragm, then it may have the risk that the diaphragm may contact and short the electrodes resulting in an electrical failure.

### 3. Physical Contradiction

PC1: We want to push against the diaphragm for creating a pressure signal but we do not want to push against the diaphragm because it causes a fuel leak between the base port and the diaphragm

PC2: Shim is needed to create a sensing cavity and shim is not needed because dimensional stability creates a cost issue

PC3. If gap is too high, sensitivity may be reduced

PC4. If gap is too short, then may be some problems related to short circuit

### 4. Diaphragm optimization

On the early designed proposal, the diaphragm design was conducted based on the understanding of the simulation model and statistical analysis; however and based on preliminary electrical tests, it was recommended to increase the dynamic range by adding more deflection to the diaphragm. Robust Engineering assessments were conducted using a dynamic zero-point proportional signal-to-noise ratio for diaphragm deflection for a High Pressure Sensor. The input signal was pressure, the output response was deflection.

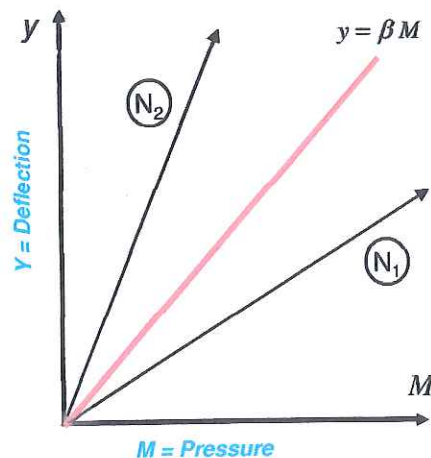


Figure 9-2. Ideal Function for diaphragm deflection optimization

The initial sensor design was developed using a series of designed experiments but a desire to reduce variability across noise conditions prompted this Robust Engineering evaluation. Diaphragm deflection was estimated using a FEA model that has correlated well in the past to physical data.

Identified were 4 control factors at three levels for evaluation such that an L-9 inner array was chosen. A compounded noise strategy of the variation of some of the factors was employed. Each treatment combination was evaluated at 5 levels of signal (Pressure).

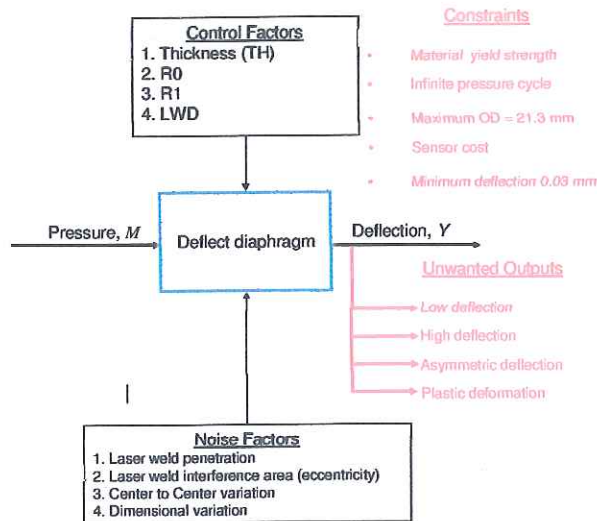


Figure 9-3. P-Diagram including Constraints and Unwanted Outputs

Analysis of the results suggested some improvements in S/N were possible but in all cases these resulted in lower levels of sensitivity. The first optimization of best S/N combination resulted in a nearly flat output – unacceptably low level of output for this sensor. The second optimization with three parameters selected for Beta improvement did not improve the result over the initial design with marginal confirmation.

	Prediction		Confirmation	
	S/N	Beta	S/N	Beta
<b>Initial</b>	-51.9	0.000027	-53.0	0.000017
<b>Optimum 1</b>	-38.2	0.000047	-39.5	0.000001
<b>Gain</b>	13.70 db		13.54 db	
<b>Improvement</b>	79%		79%	

Table 4. Optimization confirms, but does not provide sufficient deflection (Beta)

The conclusion is that this sensor was already broadly optimized such that the initial conditions will continue. The poor confirmation may be due to the highly interactive nature of the L9 inner array – future evaluations should avoid this array.

### 5. Improve Dynamic range

The larger dynamic range the better accuracy. Dynamic range is the ratio between the highest and lowest measurement values of the output signal. In the case of the HPS it was observed that during preliminary tests, the improvement of the dynamic range was necessary to obtain a better resolution as required by the customer. Some of the alternative –based on the step flat diaphragm version- was to reduce the height of the step in order to reduce the airgap between electrodes and diaphragm (Fig 9-4); however this solution actually increased the cost of the machined part.

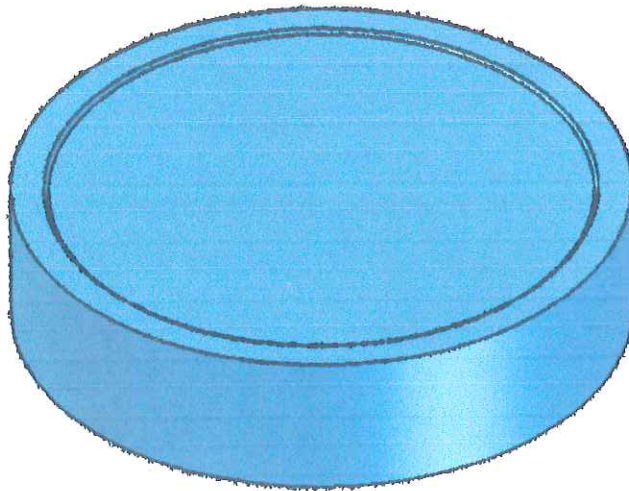


Figure 9-4. Step diaphragm used on early stages of proof of concept



A second alternative was oriented to include an additional component that cut the cost of machining process of the diaphragm (step) and provide a versatile design for different heights of the airgap. The resulting design was to include a shim on top of diaphragm (Fig 9-5) made of same material than diaphragm and baseport.

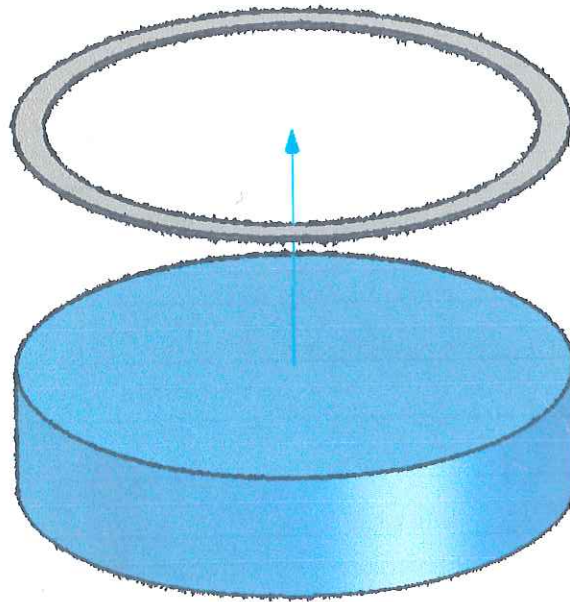


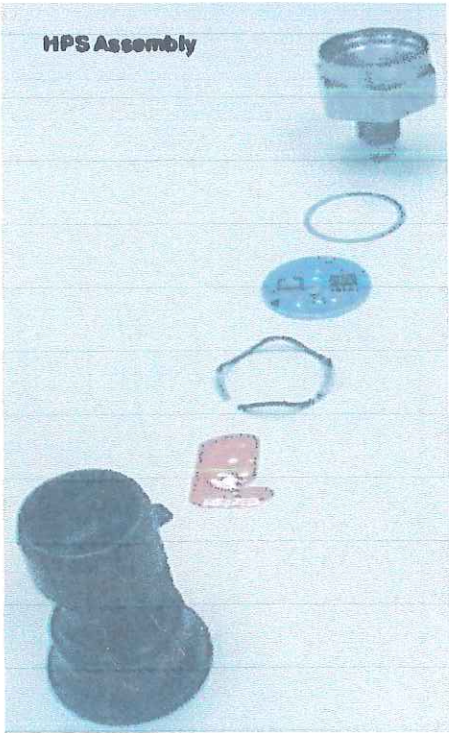
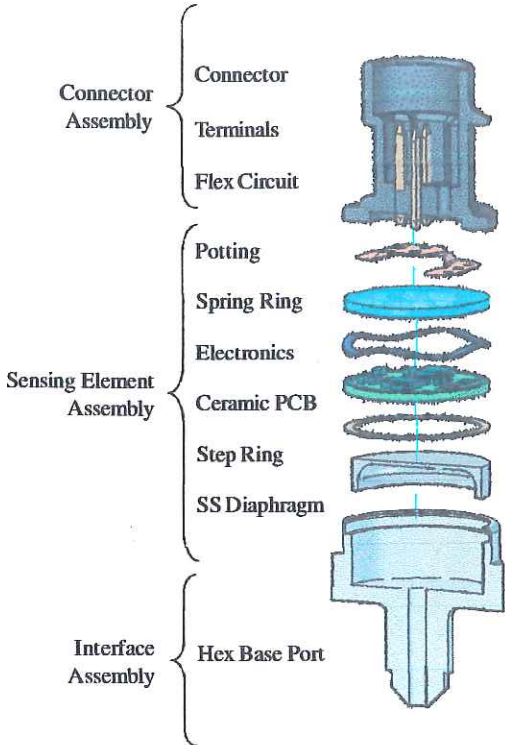
Figure 9-5. Flat diaphragm and shim option used on final design

## Chapter 10. References

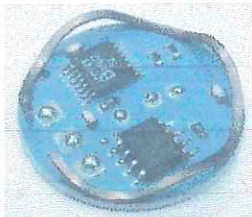
- [1] S. Timoshenko and S. Woinosky-Krieger, (1987), Theory of Plates and Shells, McGraw Hill Classic Textbook Reissue.
- [2] Robert D. Cook, Warren C. Young, (2<sup>nd</sup> Ed) Advanced mechanics of materials, Pearson
- [3] Mario Di Giovanni, (1982), Flat and corrugated design handbook, Mechanical Engineering; 11
- [4] Jacob Fraden, (3<sup>rd</sup> Ed), Handbook of modern sensors, physics, designs and applications, Springer
- [5] Yingjie Lin, Urquidi Carlos, Romo Francisco, (2008), Capacitive Pressure Sensor Patent US 7,383,737 B1
- [6] ANSYS Help, Advanced Analysis Techniques Guide, Chapter 7 on Cyclic Symmetry.
- [7] Jon Wilson, (2005), Sensor Technology Handbook, Elsevier – Newnes
- [8] Larry K Baxter, (1996), Capacitive Sensors design and application; IEEE press series on electronics technology
- [9] S.C. Mukhopadhyay · R.Y.M. Huang; (2008), Sensors Advancements in Modeling, Design Issues Fabrication and Practical Applications
- [10] Ron Schmitt; (2002), Electromagnetics explained; Newnes
- [11] Motive Magazine.(2007), Motive forum GDI
- [12] J. A. Voorthuyzen, and P. Bergveld, (1984), The influence of tensile forces on the deflection of circular diaphragms in pressure sensors, Sensors and Actuators.
- [13] J.W.S. Rayleigh, (1894), The Theory of Sound, Volumes I and II, reprinted by Dover in 1945
- [14] P.M. Morse.(1936), Vibration and Sound, reprinted by the Acoustical Society of America in 1981
- [15] Cyril M. Harris, Allan G. Piersol, (5<sup>th</sup> Ed) Shock and vibration handbook, McGraw-Hill
- [16] S. Timoshenko(2<sup>nd</sup> Ed), Vibration problems in engineering, D. Van Nostrand Co, Inc.
- [17] Werner Soedel, (3<sup>rd</sup> Ed) Vibrations of shells and plates; Marcel Dekker, Inc.
- [18] Thomas Pyzdek, (2003), The six sigma handbook; McGraw-Hill
- [19] ISO 5725-1,(1994), Accuracy (trueness and precision) of measurement methods and results -Part 1: General principles and definitions, International Standard
- [20] Lion Precision, (2008), Capacitive Sensor Operation and Optimization, Technote Lion Precision.

## APPENDICES

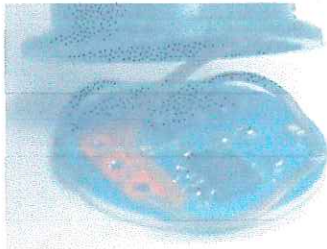
Appendix A. High Pressure Sensor schematic



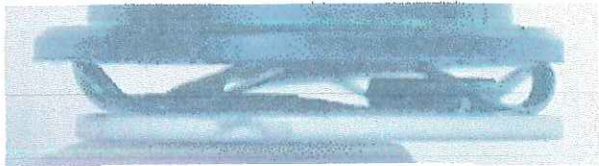
Base port-Diaphragm assembly



Circuit Board - Spring ring



IC - Flex Circuit Connection



Vertical stack up

Appendix B. Patent No. US 7,383,737 B1



**United States Patent**  
Inventor

Patent No. US 7,383,737 B1  
Date of Patent: Jun. 16, 2008

**CPAP/PEEP/STAPLE SYSTEM**

Inventor: **David A. Wilson, II, San Diego, Calif.**  
Assignee: **Wilson Medical, Inc., San Diego, Calif.**

**Background**

CPAP/PEEP/STAPLE SYSTEMS are used to treat various respiratory conditions, such as sleep apnea, chronic obstructive pulmonary disease (COPD), and asthma.

**Summary**

The present invention provides a CPAP/PEEP/STAPLE SYSTEM that includes a mask, a circuit, and a control system.

**Detailed Description**

The CPAP/PEEP/STAPLE SYSTEM includes a mask assembly (10) and a circuit assembly (20). The mask assembly includes a mask (11) and a headgear (12). The circuit assembly includes a control system (21) and a power source (22). The control system is configured to control the flow of gas through the mask and the circuit.

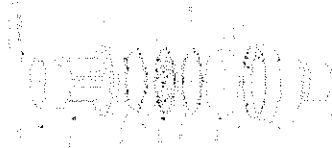


FIG. 1

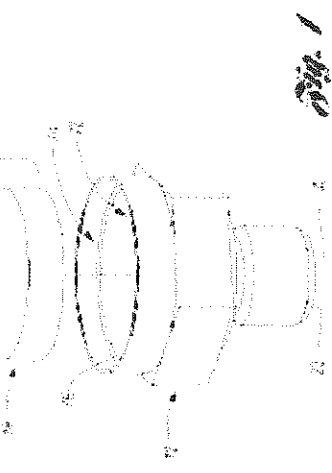


FIG. 2

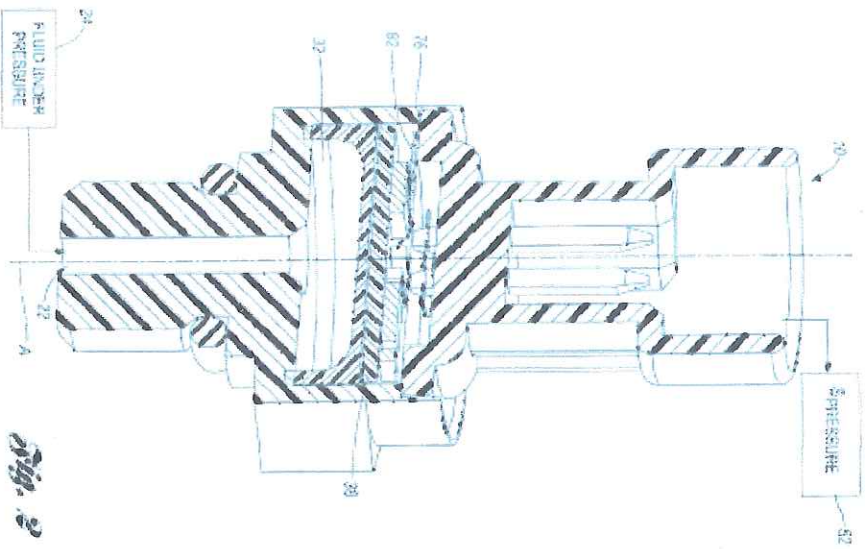


Fig. 2

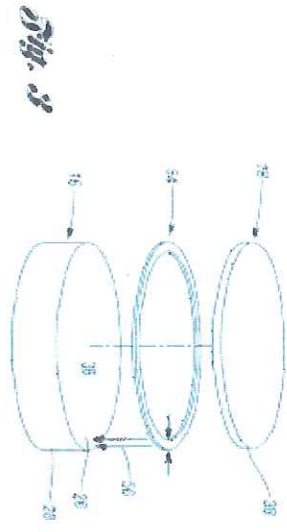


Fig. 3

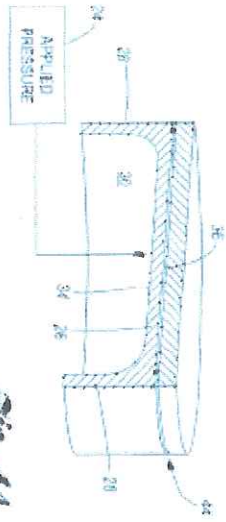


Fig. 4



Fig. 4B

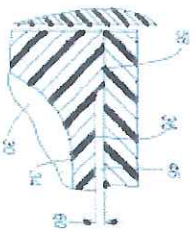


Fig. 4C

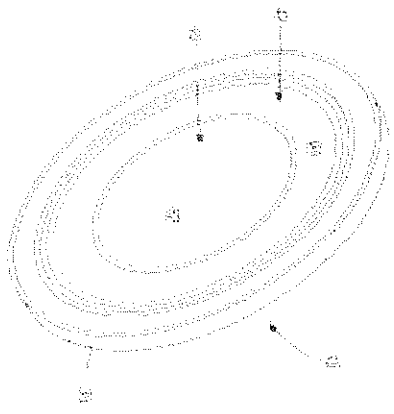


Fig. 3



Fig. 4

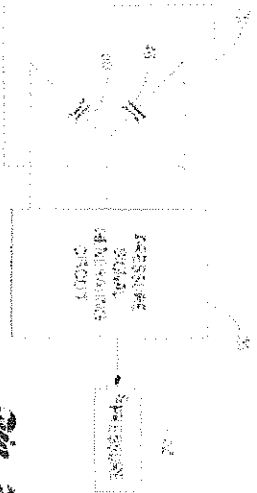


Fig. 5

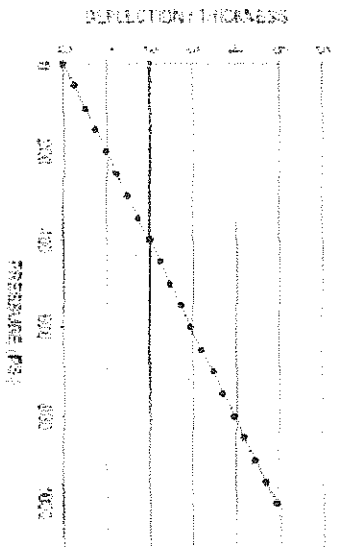


Fig. 6

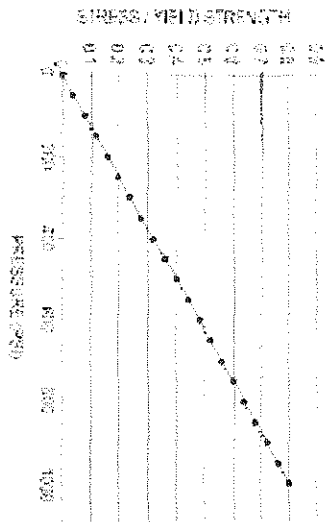


Fig. 7

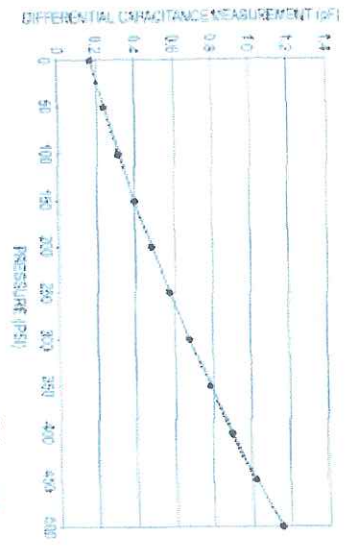


Fig. 10

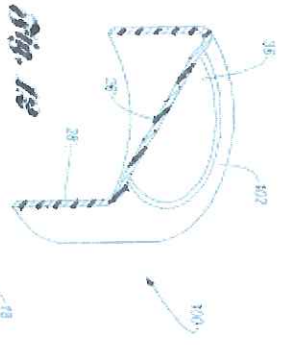


Fig. 12

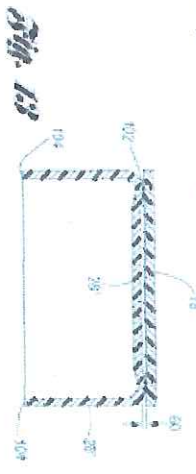


Fig. 13

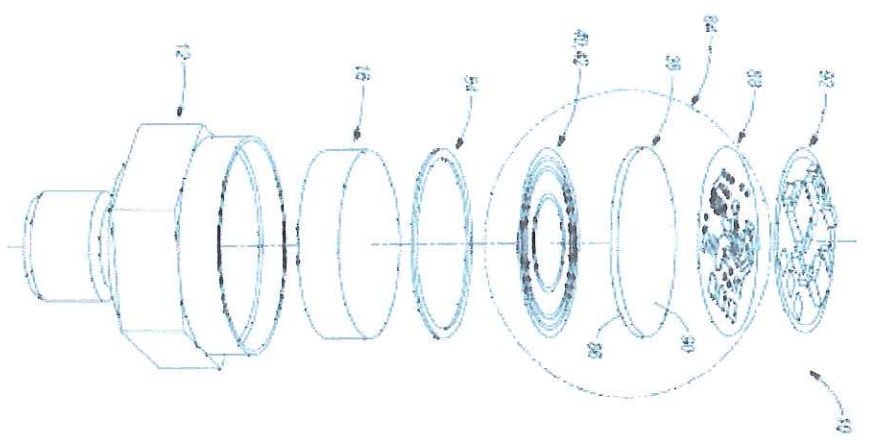


Fig. 11





Fig. 11A

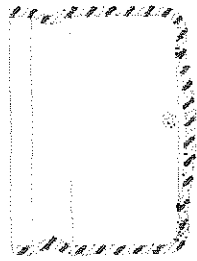


Fig. 11B

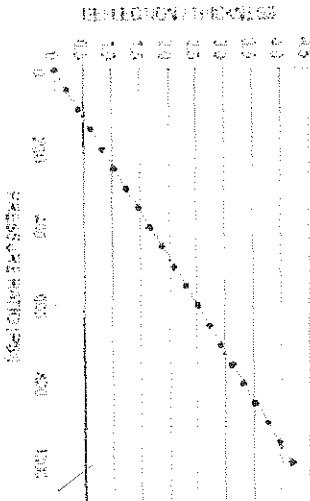


Fig. 11C

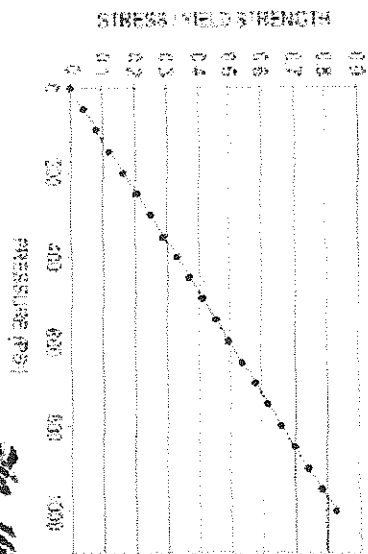


Fig. 11D

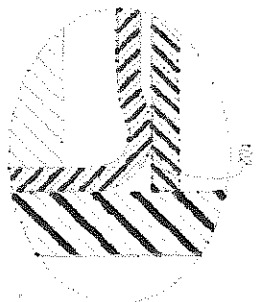


Fig. 11E

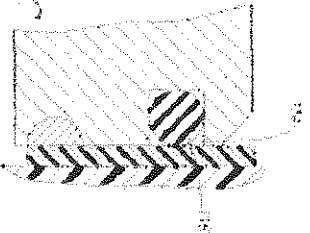


Fig. 11F

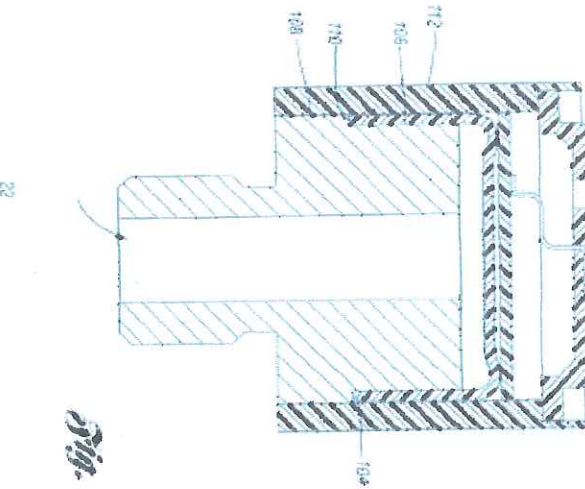


Fig. 17A

### CAPACITIVE PRESSURE SENSOR

#### TECHNICAL FIELD

The invention pertains in general to sensors, and more particularly to capacitive pressure sensors.

#### BACKGROUND OF THE INVENTION

In the automotive industry, it is frequently necessary to know the magnitude of hydrolic pressure in a container or other a pressure line. Current technologies for pressure measurement sensors include piezoelectric technology implemented using thick film, thin film and MEMS which involves, for example, bonding a silicon chip to the top surface of a casting member.

Alternatively, it is known to employ capacitive methods, for example, in MEMS and/or discrete technologies, as set forth in U.S. Pat. No. 5,638,780 entitled "CAPACITIVE PRESSURE TRANSDUCER WITH AN INTEGRAL DIELECTRIC SENSOR FOR CHECKING VALVE DISPOSITION" issued to Peter Chou, et al. This device includes a pressure transducer that includes a transducer element and a conductive layer that includes both a piezoelectric and a piezoresistive layer. The variable of which one electrical property is affected is the piezoelectric property of the piezoelectric layer. The variable of which the other electrical property is affected is the piezoresistive property of the piezoresistive layer. The device described in Chou, however, is rather complicated and includes an increased number of parts. Currently, the conventional art of capacitive sensing requires elaborate manufacturing processes and an increased number of parts to assemble the sensing element. Moreover, these sensors also have a deteriorating behavior as not being able to effectively seal high pressures. In addition, conventional sensing elements are generally not compatible with a wide range of media (i.e., the fluid whose pressure is being sensed). There is therefore a need for a sensor that maintains or overcomes the shortcomings set forth above.

#### SUMMARY OF THE INVENTION

A sensor is associated with this invention provides a simplified manufacturing process and assembly procedure. The simplified and complex manufacturing process described in the Background. Additionally, embodiments of the present invention provide a configuration with a reduced number of parts, fewer steps that can be thereby improving reliability. Additionally, the simplified configuration provides for a less expensive sensor. Further, a sensor according to the present invention includes a mechanism that provides for greater flexibility in engineering the sensor diaphragm for different pressure ranges, media compatibility and material selection of which improve the cost effectiveness of the sensor.

Pressure sensors according to the invention includes a base-pipe, a membrane having a diaphragm and a sensing element which is a piezoresistive layer. The base-pipe includes an opening equal in length to the diameter of the base-pipe. The diaphragm is a membrane having a pressure in the center and the outer edge. The sensing element is applied to the inner side wall which defines an inner opening of the diaphragm. The diaphragm is characterized by a protrusion which has an angled 15-degree in cross-section. The diaphragm is angled relative to the base-pipe to stabilize the membrane in direct communication with the fluid opening of the base-pipe to thereby form a fluid pressure

US 7,383,737 B1

entry. The base wall of the diaphragm has a working surface facing the fluid pressure entry and an opening. The sensing surface.

The sensing diaphragm body includes an underlying substrate layer (structure) having a center electrode and a ring electrode both having a ring and spaced apart from the sensing element of the diaphragm by a space to form an air gap. The sensing element is a piezoresistive layer applied to the inner surface of the diaphragm and the ring electrode and the substrate are connected to ground. Changes in pressure in the fluid pressure entry proportionally result in variations in the capacitance of the first capacitor, with potential errors inherent in the second capacitor. Finally, the pressure signal generating circuit is responsive to variations in the capacitance of the first and second capacitors, preferably measured in a differential mode, to generate a pressure signal indicative of the fluid pressure.

Other embodiments are presented, including those where the sensor comprises a ring ring or an integral step on the diaphragm surface.

#### BRIEF DESCRIPTION OF THE DRAWINGS

The present invention will now be described by way of example, with reference to the accompanying drawings. FIG. 1 is an exploded view of the inventive capacitive pressure sensor in an assembled state.

FIG. 2 is a partial, perspective view of the sensor of FIG. 1 in an assembled state.

FIG. 3 shows a greater detail of a sensing diaphragm body of FIG. 1.

FIG. 4A-B are cross-sectional views of the diaphragm and sensing element body in an assembled state.

FIG. 5 is a perspective view of the sensing element body of FIG. 1 showing the center and ring electrodes.

FIG. 6 is a cross-sectional view of the diaphragm of FIG. 1 showing an approximation of a fluid pressure resulting in a deflection.

FIG. 7 is a perspective diagram of the sensor of FIG. 1 showing a full range of deflection for determining a differential capacitance corresponding to the pressure.

FIG. 8 is a perspective view of the present invention showing the air gap and the pressure diaphragm, corresponding to the air gap diameter of the present invention.

FIG. 9 is a cross-sectional view of the sensing element which includes a ring electrode and a center electrode, both having a ring and spaced apart from the sensing element of FIG. 1 by a space to form an air gap. FIG. 10 is a perspective view of the sensing element of FIG. 9 showing a detail of the ring electrode.

FIG. 11 is a perspective view of the sensing element of FIG. 9 showing a detail of the center electrode.

FIG. 12 is a perspective view of the sensing element of FIG. 9 showing a detail of the center electrode. FIG. 13 is a perspective view of the sensing element of FIG. 9 showing a detail of the center electrode.







**COMPUTATIONAL SIMULATION FOR DEFLECTIVE DIAPHRAGM USED ON CAPACITIVE PRESSURE SENSOR**

Franklin David Paris  
 GEOMET - 2072 - CONTACT  
 At: P.O. Box 24, La Crosse, WI, 54601  
 Telephone: 608/785-3800  
 Computer: Com. Manager  
 E-mail: frankd@com.net

**Abstract:** Computer simulation is the order of the day for design of both inductive and capacitive diaphragm sensors. One of the applications is the capacitive sensor which uses a thin diaphragm to sense the change in the capacitance of a capacitor under pressure loading. This is the case for the sensor design. One is asked to design a sensor which will have a certain deflection (strain) in the diaphragm or the reference to measure the diaphragm pressure. The order of the day is to design a sensor which will have a certain deflection in the diaphragm.

The diaphragm (1) is used to sense the change in the capacitance of a capacitor under pressure loading. This is the case for the sensor design. One is asked to design a sensor which will have a certain deflection in the diaphragm or the reference to measure the diaphragm pressure. The order of the day is to design a sensor which will have a certain deflection in the diaphragm.

**Keywords:** Pressure sensor, diaphragm, capacitive, simulation, design of experiment (DOE)

**1. INTRODUCTION**

Creation of sensors of pressure based on deformation of thin plates is a complex task. The design of such sensors based on deformation in a diaphragm, along the line of the new product, is the case of a new sensor. The design of such sensors based on deformation in a diaphragm, along the line of the new product, is the case of a new sensor. The design of such sensors based on deformation in a diaphragm, along the line of the new product, is the case of a new sensor.

**2. THE CASE**

Membrane sensor is well known. For the membrane small transverse deflection  $w_{max}$  at the center of the disc (see Fig. 1) fixed center also under uniform applied pressure  $q$  is given by the equation (Timoshenko, 1957):

$$w(r) = \frac{q r^4}{64 D} \left[ 1 - \left(\frac{r}{a}\right)^4 \right] \quad (1)$$

where  $r$  is the radius of the disc  $r = 0, 0 \leq r \leq a$

$$w_{max} = \frac{q a^4}{64 D} \quad (2)$$

where  $a$  is the radial position of the deflection  $D$  is defined and is given by the general equation for a specific diaphragm with fixed edges without residual stress in special case for  $\nu = 0$  and  $\nu = 0.3$  (see Appendix A) following definitions:

$$D = \frac{E h^3}{12(1-\nu^2)} \quad (3)$$

$E$  is the Young's modulus,  $h$  is the thickness of the diaphragm and  $\nu$  is Poisson's ratio

The total stress in the diaphragm is given by (Timoshenko, 1957; Blevins, 1995):

$$\sigma_r = \frac{3 q a^2}{8 h} \left( \frac{r^2}{a^2} - \frac{r^4}{a^4} \right) + \frac{1}{4} \frac{q a^2}{h} \quad (4)$$

$$\sigma_\theta = \frac{3 q a^2}{8 h} \left( 1 - \frac{r^2}{a^2} \right) + \frac{1}{4} \frac{q a^2}{h}$$

The conditions can be calculated by:

$$\sigma = \int \epsilon(r) \frac{d\sigma}{dr} \quad (5)$$

where  $\epsilon$  is the strain along the diaphragm (for  $\nu = 0$  it is very close to  $D$ )  
 $\epsilon$  is the diaphragm constant of stress  $\epsilon = \frac{1}{E} \frac{d\sigma}{dr}$   
 $D$  is the disc diameter between the electrodes.

**3. PRINCIPLE OF OPERATION**

The basic of the operation of the sensor is given related to the diaphragm membrane displacement between two electrodes that under the pressure, there is no initial displacement while the sensor is in pressure state. The change in diaphragm between electrodes is the cause causing a force along the axis of the membrane as electrodes appear in the center located in Figure 1. Figure 1 shows the sensor design to push the design and with good and robust diaphragm. The pressure sensor consists of the understanding of the sensor and design transmission to transfer and calculate a thin diaphragm deflection.



Fig. 1. Example of operation. Gap variable versus pressure, membrane sensor stress versus pressure

## 4. COMPUTER SIMULATIONS

In order to determine the best design for the objective displacement field under dynamic loading, a 3D finite element analysis of a laminar or composite pressure vessel is important due to the fact that stress distribution and strain will depend on the shape of displacement of the strain.

The objective displacement pressure and stress distribution obtained for different displacement designs in the uniaxial field from a non-linear 3D commercial software (ANSYS) and numerical analysis (FEM) based on dynamic loading to carry out a finite element analysis for further development under stress or strain displacement design. Figure 3 includes types of the main displacement for the displacement design. The design, however, and their results in different shapes because they are related to the displacement method (field region) and a function of displacement or a shape of the field may be considered for the analysis.



Fig. 3. Cross section representation of internal displacement and stress design.

A 3D finite element stress analysis of the displacement was performed using several other numerical elements for different displacement designs and compared their characteristics when the main design factors to consider were:

1. Material selection  
Type of displacement  
Pressure behavior
2. Displacement parameters  
Field shape  
Displacement  
Displacement stress
3. Boundary conditions  
Edge condition  
Edge condition  
Temperature change

As a rule of thumb for dynamic analysis, the maximum stress on the part should be about 50% of the yield strength in order to obtain good design life. To account for material properties and yield stress variation, the maximum recommended pressure load should be the half of the yield stress of the material used and oriented in the same direction. It is important to ensure that the boundary conditions will also affect the stress and displacement field. For this analysis, it is considered a top welded seam on the pressure vessel of the displacement or stress distribution design. This consideration provides additional to the displacement and stress distribution can be analyzed as "displacement" dependent for different field parameters.

There is an additional concern related to the Material Properties based on speed of concept with results that is a "stress" applied to the field region which can not be taken as a single property during simulation due to the fact that both relative pressure stress field should be performed in order to provide a maximum and minimum yield strength values.

### 4.1 POST-DEFORMATION

It would also be possible to perform a 3D FEA analysis of the results since the simulation and output of a 3D simulation. However, due to the complexity of the 3D analysis, which stress performed in this analysis is available in the literature. For various models used in 3D, it is suggested to use the literature reference such as [20, 21].

### 4.2 RECONSTRUCTION

Once defined the displacement and during construction and speed of concept, it is also recommended to improve the performance of the displacement by using one of the following references [20, 21] (Figure 4):

1. Constant displacement
2. Surface finish
3. Construction method

### 4.3 RESULTS

Based on FEA simulation results for stress distribution and structural analysis (SAS), it can be observed that:

1. Increasing the load pressure carrying capability will decrease the deformation of the displacement.
2. Increasing the main stress to displacement and pressure pressure field and reduction of the displacement.
3. Increasing provides enough structural support in order to avoid deformation in the center and outer displacement and displacement.
4. Stress displacement is expected to be lower along displacement.
5. Having a good alignment of the displacement, the stress concentration at the outer stress or at the field position will decrease.
6. It is observed that if field pressure increases, the maximum stress location is shifted from the center of displacement to the outer stress (wall thickness) and the stress concentration. So, it is recommended to increase the wall thickness to improve the displacement carrying capability.
7. Inner stress and outer stress displacement has the same behavior, however, need to be considered according to yield point of the material used.
8. Refer to Figure 2 for model results. It is recommended to use a 3D provided geometry (3D) design structure of the cylinder structure for further stress analysis. With only 1/4 of the part analyzed in the only corner under top stress region and 1/4 region. There will be a lot of stress due to the part symmetry. After stress analysis, it is observed that the maximum or minimum displacement, the design may or may not change for the particular case the main condition was not considered.

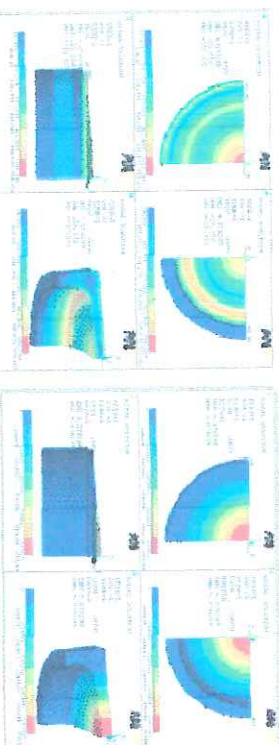


Fig. 4. Stress distribution for different Maximum stress is considered as a function of displacement and construction method.

Fig. 5. Displacement for different Maximum stress is considered as a function of displacement.

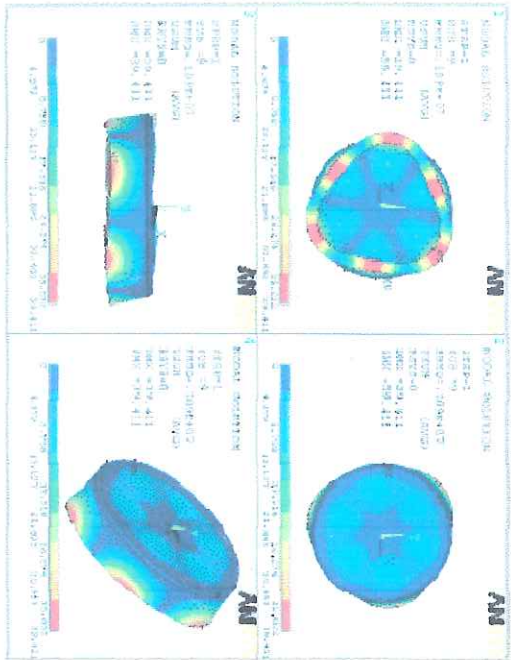


Fig. 1. 3D-dol. Equations. Defined data for diamond ring. Recommended to analyze the whole diamond to avoid the influence of angle and provide an accurate solution.

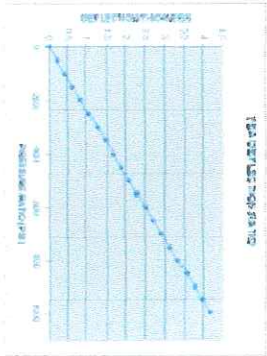


Fig. 6. Stress ratio (0 - 1000 Pa) to Defective positions

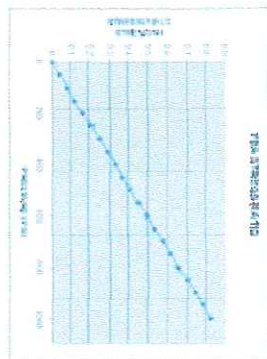


Fig. 7. Stress ratio (0 - 1000 Pa) to Yield Strength Stress

As mentioned above, the testing calculations were carried out based on Design Of Experiments (DOE) as shown on figures 5 and 6 under the summation axis.

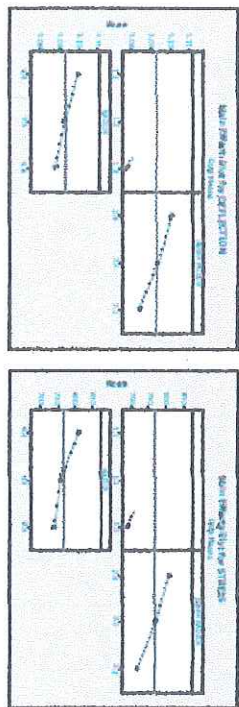


Fig. 8. Also other plots for Deflection and Stress. It can be observed that Deflection plots a significant impact for the deflection behavior.

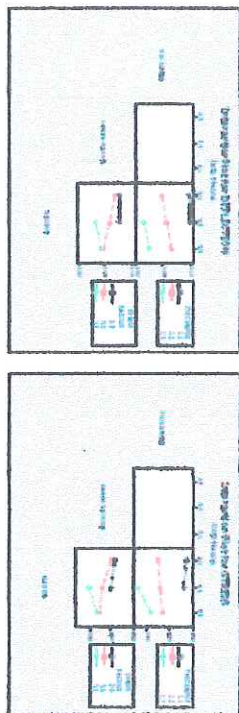


Fig. 9. Interaction plot for Deflection and Stress for distance (Pa). There is not significant interaction between factors.

#### REFERENCES

- ANSYS. ANSYS Help (Palanis 1). Advanced Analysis Technology Guide. Chapter 7 on Cyclic Symmetry. Shiva Di. Ghomai (1972). *Form and Formulas for Engineers*. CRC Press.
- Wilson P. Easa. Fernando Silva. Javier H. South. David W. Swimmer (1993). *A new analytical solution for diamond ring deflection and its application to a surface-levelling precision sensor*. Florida National Laboratories. Alliquipueva, FL.
- Teada Padua. (2001). *Handbook of modern sensors: design and applications*. Springer.
- Yungfa Lin. Cheng Chen. Feiya Francisco. (2006). *Capacitive Pressure Sensor*. Patent 677,733, 737-82.
- S. Timoshenko and S. Woinowsky-Krieger. (1957). *Theory of Plates and Shells*. McGraw Hill.